Using Vegetable Oils for Biofuel Accelerates Tropical Deforestation and Increases Carbon Emissions

Tzu-Hui J. Chen[1], Richard J. Sexton[1], and Aaron Smith[2]

[1]Department of Agricultural and Resource Economics, University of California, Davis CA 95616, USA

[2]Department of Agricultural and Resource Economics, University of California, Berkeley, CA 94720, USA

Abstract

Biofuels are promoted worldwide as a strategy to replace fossil fuels and cut greenhouse gas emissions. However, their climate benefits are uncertain because biofuel production can induce deforestation and other land use change that causes carbon emissions (1; 2). Here we show that global demand for biomass-based diesel fuel between 2002 and 2018 drove the conversion of approximately 1.7 million hectares of forest to oil palm in Indonesia and Malaysia, which is about one-fifth of the total forest-to-palm expansion during this period. Using econometric models and high-resolution satellite data, we demonstrate that biomass-based diesel demand raised palm oil prices, which in turn accelerated deforestation, primarily in natural forests. The associated land-use change released more than one gigaton of CO_2, giving biomass based diesel higher carbon emissions per megajoule than that of fossil diesel. These findings indicate that biofuels derived from vegetable oils have likely increased, rather than reduced, global emissions, and highlight the urgent need to shift renewable fuel policies away from crop-based feedstocks.

Main

Government policies that encourage biofuels aim to cut carbon emissions, but they may also accelerate deforestation. Biomass-based diesel (BBD) made from vegetable oils has grown rapidly as a substitute for petroleum diesel, accounting for about 17% of global vegetable oil use in 2023. Yet, converting forests and other native vegetation to cropland produces roughly 10% of all human-induced carbon emissions (3), raising doubts about the climate benefits of BBD fuels. Understanding how biofuel expansion affects land use and emissions is therefore critical to assessing whether BBD truly advances, or undermines, climate goals (2; 4).

Palm oil, the most widely used vegetable oil worldwide, is an important feedstock for BBD and a major driver of tropical deforestation. Most palm production occurs in Indonesia and Malaysia, where forest loss has been extensive (5; 6). For example, Borneo's forest cover declined by 14% from 2001 to 2017, largely driven by the expansion of palm plantations (7). Although several countries have restricted palm oil in biofuel policies because of deforestation concerns, rising BBD demand for other vegetable oils can still raise palm oil prices, since these oils are close substitutes (8; 9; 10). Higher prices, in turn, incentivize further forest conversion. This market-driven mechanism—where rising biofuel demand indirectly induces deforestation—is known as indirect land-use change (ILUC).

Despite the policy relevance of ILUC, empirical evidence remains scarce (2), especially for the rapidly expanding BBD sector. Most existing studies on ILUC rely on ex-ante modeling approaches, such as computable general equilibrium (CGE) models, yielding mixed results (15; 16; 17; 18). These broad discrepancies largely reflect modelers' different assumptions and choices of parameters, such as consumer behaviors, the degree of intensification, and substitutability among different agricultural commodities (19; 20). Moreover, many models do not consider unmanaged land and are unable to predict the accurate location of the land use changes, which leads to biased and uncertain estimates of emission

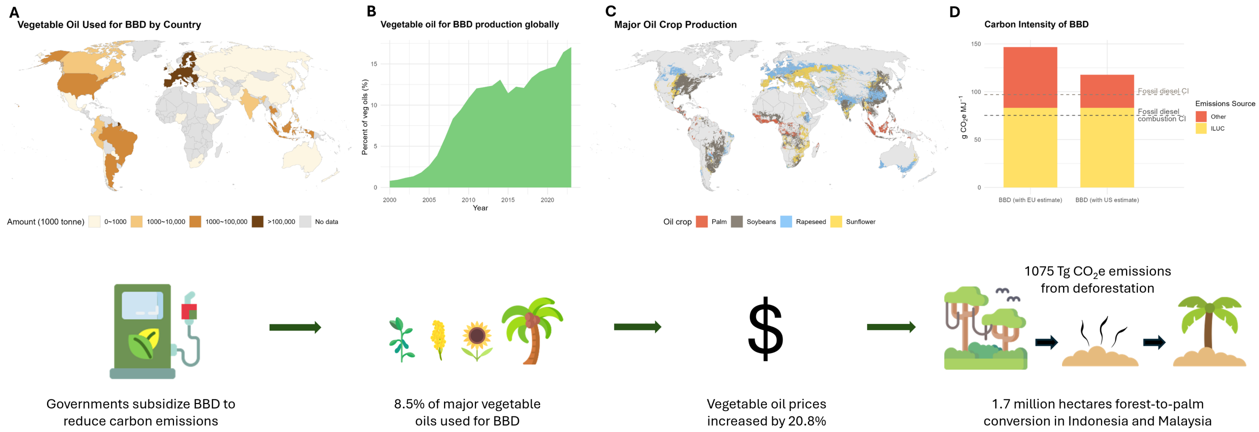

Figure 1: Global use of vegetable oils for biomass-based diesel (BBD) and resulting land use change and carbon emissions. **A.** Vegetable oils used for BBD by country, 2000-2023. Source: OECD. **B.** Global share of vegetable oils used for BBD production, showing that an average of 8.5% of vegetable oils were used for BBD between 2002 and 2018. Source: OECD. **C.** Major oil crop production regions in 2010. Source: (11). Our analysis estimates that BBD use from 2002–2018 increased vegetable oil prices by 20.8%. **D.** Estimated carbon intensity of BBD from ILUC, based on this study's analysis, compared to fossil diesel and other lifecycle emissions from US and EU government data (12; 13; 14). Our analysis further estimates that BBD use during this period led to 1.7 million hectares of forest-to-palm conversion in Indonesia and Malaysia, releasing approximately 1,075 Tg CO_2e.

factors (16; 20).

Here, we provide empirical evidence linking global BBD expansion to deforestation and associated carbon emissions. Our econometric approach reduces reliance on model assumptions and reveals causal relationships between global biofuel consumption, palm-oil prices, and observed land-use change. We use remote sensing data to detect the actual location and magnitudes of forest-to-palm conversion in Indonesia and Malaysia from 2002 to 2018. Using high-resolution remote sensing data to detect deforestation also lowers the uncertainty involved in carbon emission calculations, enables analysis across land with varying environmental values, and overcomes the limitation of tracing illegal deforestation activities in government data.

We integrate a series of econometric analyses, as illustrated in Figure 1. First, we quantify how global BBD policies affect palm oil prices by estimating econometric demand and supply models for oil palm and other major oil crops: soybeans, rapeseed (canola), and sunflower. Next, we estimate the effect of palm oil price fluctuations on deforestation using remote sensing data (21; 22; 23) and panel econometric techniques. We generate 32,305 grid cells (9km × 9km resolution) covering the years 2002–2018. To estimate carbon emissions from forest-to-palm conversion, we integrate spatial data on biomass (24), peatland location (25), palm plantations (22), forest cover (21), and initial forest type (23). Finally, we combine the forest-to-palm and demand/supply estimates to quantify the overall impact of BBD policies on deforestation and associated carbon emissions.

Our analysis reveals that global BBD consumption from 2002 to 2018 has led to higher palm oil prices, contributing to the conversion of forests to oil palm plantations in Indonesia and Malaysia. Analysis of the regions where forest loss is linked to higher palm oil prices shows that expansion of oil palm plantations primarily leads to the conversion of natural forests, with little effect on planted forests or agroforestry. The carbon emissions from this deforestation likely exceed the emissions from petroleum diesel. Furthermore, the high substitutability among vegetable oils suggests that policies targeting only palm oil in BBD production are ineffective in reducing deforestation. These findings underscore the importance of accounting for ILUC effects in policy design and highlight the urgent need to shift biofuel strategies away from crop-based feedstocks.

Biomass-based diesel demand raises palm oil prices globally

Many governments subsidize BBD, boosting demand for vegetable oils and driving up prices for both palm oil and its substitutes, such as soybean, rapeseed, and sunflower oil. The magnitude of the price increase depends on the extent to which other users are willing to reduce consumption (demand elasticity) and the extent to which production expands (supply elasticity). From 2002 to 2018, on average, around 8.5% of global vegetable oil consumption was used annually for BBD. Using our estimated demand and supply elasticities, we find that this BBD-driven demand shift raised palm oil prices by roughly

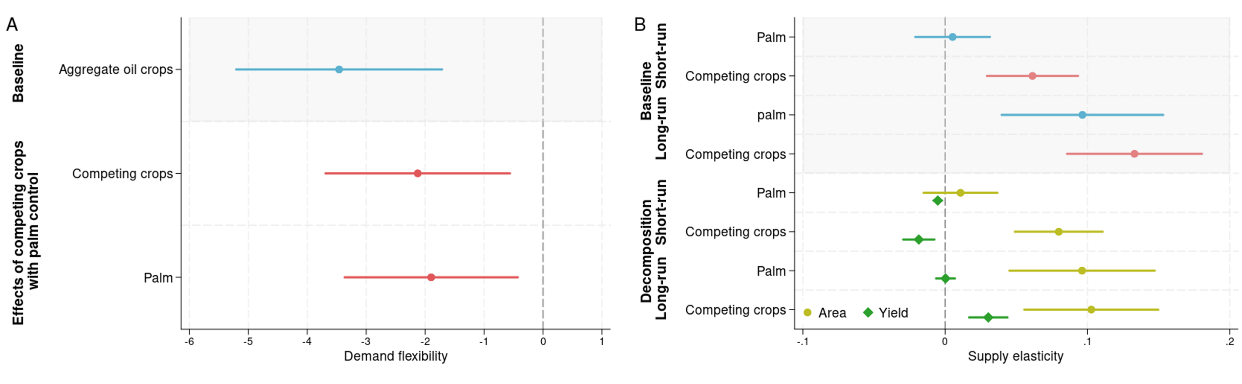

Figure 2: Estimated demand and supply responses to palm oil prices. **A.** Demand flexibility: Row 1 shows the baseline estimate of effects of aggregate oil crop production (oil palm fruit, soybeans, rapeseed, and sunflower) on palm oil prices, while rows 2–3 present the effects of competing oil crop production (soybeans, rapeseed, and sunflower) on palm oil prices, controlling for palm production. **B.** Baseline supply price elasticities with respect to palm oil prices: short-run palm (row 1), short-run competing crops (row 2), long-run palm (row 3), and long-run competing crops (row 4). Decomposition of supply elasticities into area and yield responses (rows 5-8). The estimates are from regressions with a flexible time trend of restricted cubic splines with 5 knots. Circles denote regression point estimates; lines represent 90% confidence intervals.

20.8% relative to business-as-usual (BAU) levels (90% confidence interval: [12%, 27.9%]).

Figure 2A row 1 demonstrates the estimated demand flexibility (inverse demand elasticity), indicating that, on average, a 1 percent decrease in the production of vegetable oils (oil palm fruit, soybeans, rapeseed, and sunflower) results in a 3.5% increase in palm oil prices (90% confidence interval: [1.7%, 5.1%]), corresponding to a demand elasticity of -0.29 for oil palm. Supplementary Information Section A contains further details on these findings and shows that the estimates are similar across various time trend specifications.

The baseline demand model imposes a common elasticity across all four oils, but some countries do not use, or are actively reducing their use of, palm oil for BBD. For example, the US does not produce biofuels made with palm oil (26), and the EU has adopted policies to phase down palm oil use (27). If the four oils were not close substitutes, then biofuel policies targeting other vegetable oils would have little impact on palm oil prices and would allay concerns of forest-to-palm conversion. To explore this possibility, we separate demand for oil palm fruit from the three competing oil crops (soybeans, rapeseed, and sunflower). The response of palm prices to production shocks in the competing oil crops is very similar to the estimated response to palm production shocks (Figure 2A rows 2-3). This result indicates that lower production of other oil crops raises palm oil prices even after controlling for palm production. These findings confirm that palm oil is highly substitutable with other major oil crops, a finding consistent with prior studies (8; 9; 10) and with the cointegration results in the Supplementary Information Section B. Thus, a policy to restrict palm oil alone in BBD production is unlikely to significantly curb deforestation or the associated carbon emissions.

If oil crop production could respond easily to an increase in demand from BBD, then palm oil prices would not increase sharply. To assess this possibility, we estimate supply price elasticities. The short-run supply elasticity of oil palm is small and not statistically different from zero (Figure 2B, row 1), indicating that palm production cannot smooth price increases immediately. This result is expected given that oil palm is a perennial crop that requires about four years from planting before fruiting (28; 29). By contrast, the short-run supply elasticity of the three competing oil crops is statistically different from zero (Figure 2B, row 2), suggesting that these annual crops can offset part of a cooking-oil demand shock relatively quickly. In the long run (>6 years), palm production also responds to rising prices ; a 1% price increase leads to a 0.1% production increase (90% confidence interval: [0.04%, 0.15%], Figure 2B, row 3). The long-run elasticity of the competing crops implies that a 1% price increase leads to a 0.13% production increase (90% confidence interval: [0.09%, 0.18%], Figure 2B, row 4), which is slightly larger than the short-run value, suggesting that some production adjustments take time. Further details on the long-run results are provided in the Supplementary Information Section C.

An additional consideration is whether higher prices encourage farmers to increase output primarily through intensification on existing cropland or through cropland expansion. If the response is mostly to intensify production, the carbon emissions from land-use change would be less severe. The assumption of a strong intensification response underlies some CGE models studying ILUC (30; 20). We decompose the supply response into area and yield components. The baseline estimate indicates that yield improvements from palm are small and insignificant (Figure 2B, row 7). For the competing crops, approximately 77% of the supply response comes from area expansion, whereas yield improvements account for only 23% (Figure 2B, row 8). Although the precise shares vary across time model specifications (Supplementary Information Section C), the general pattern is clear: area responses dominate yield responses for both palm and the competing oil crops.

Higher palm prices accelerate deforestation in Indonesia and Malaysia

Higher palm oil prices increase the attainable revenue from deforesting to produce palm. We find that an increase in attainable revenue of $1,000 (USD) per hectare corresponds to an additional 9.4 hectares of deforestation for palm plantations in the average cell in Indonesia and Malaysia (90% confidence interval: [7.3, 11.5]), amounting to approximately 300,000 hectares across the entire region (Figure 3A, row 1). For reference, between 2002 and 2018, the average annual attainable revenue was $1,934 per hectare, while the average annual deforestation for palm plantations was 15.48 hectares per cell.

This estimate is similar across specifications and alternative channels, including different region and trend controls (Figure 3A, rows 2-3), reverse causality tests (Figure 3A, rows 4-6), weather controls (Figure 3A, rows 7-9), and different deforestation pressure due to attainable yields (See detailed discussion in Supplementary Information Section D).

To assess the environmental damage from deforestation, we decompose the deforestation response by forest type. We separate the forest into natural forests without management, natural forests with management (e.g., selective logging, logging, or other human activities), planted forests, and agroforestry (23) and re-estimate our main regression model for each subset (Figure 3B, row 1). Results show that revenue increases have the strongest deforestation effects in unmanaged natural forests, followed by managed

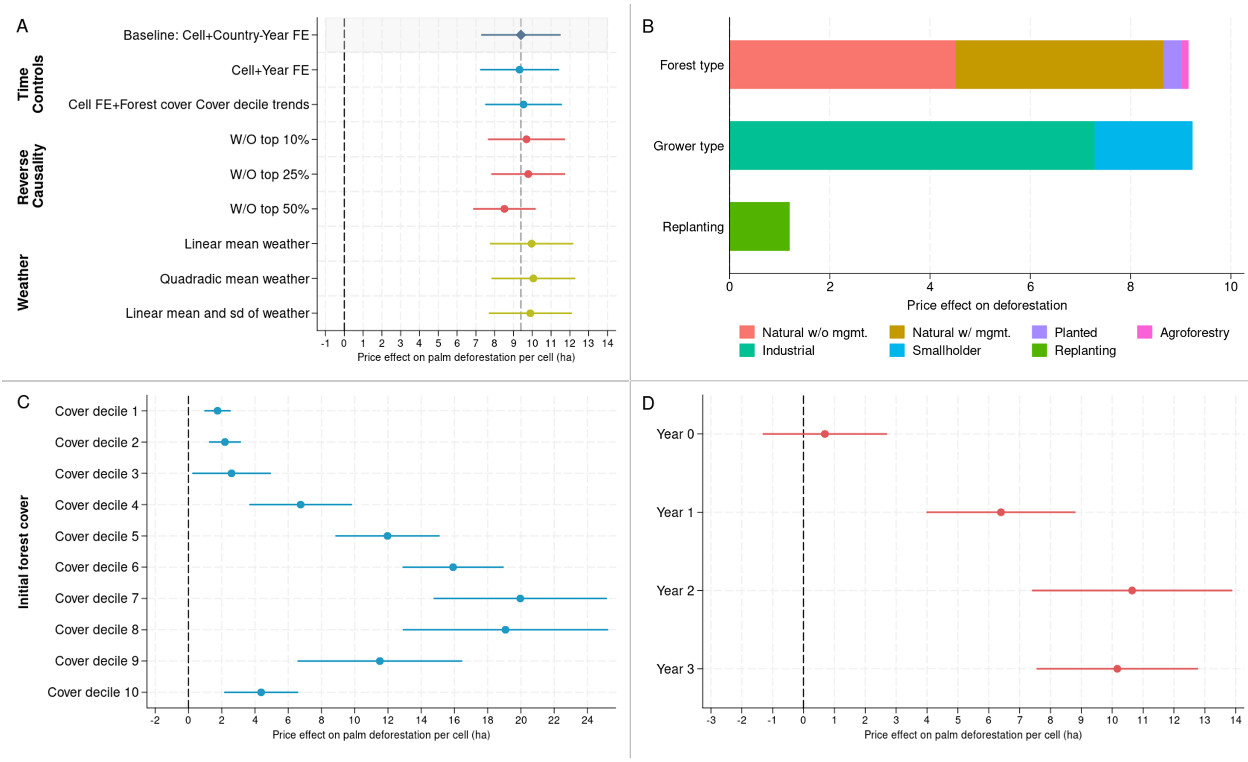

Figure 3: Estimated effects of a $1,000/ha increase in attainable revenue on deforestation area (hectares per cell). Circles indicate regression point estimates; lines show 90% confidence intervals. **A.** Baseline estimate (row 1) and robustness to alternative specifications: different time controls (rows 2–3), reverse causality, i.e., whether expectations of future palm expansion affect prices (rows 4–6), and weather controls (rows 7–9). **B.** Decomposition of baseline effects by forest and grower types: natural forests without management, natural forests with management, planted forests, agroforestry (row 1), industrial plantations vs. smallholders (row 2). Also shown are price effects on replanting (row 3). **C.** Heterogeneous effects by initial forest cover deciles. **D.** Cumulative deforestation responses over ensuing years to revenues.

natural forests. The effects are small for planted forests and agroforestry. These results imply that palm growers preferentially expand into natural forests rather than replacing existing planted areas (28). We do not classify existing palm plantations as forests, as replanting does not alter land-use-related carbon stocks in the long run. Separately, we estimate the replanting responses to palm oil attainable revenue and find that growers increase replanting when attainable revenues are high (Figure 3B, row 3), likely reflecting expectations of future price strength and the incentive to replace older trees with younger, higher-yielding palms.

We also explore heterogeneity by grower type, using the classification of (31) (Figure

3B, rows 2). This classification distinguishes industrial from smallholder plantations based on plantation size, geometric patterns, tree structure, and stand age uniformity. Our results show that industrial growers are substantially more responsive to palm oil prices, contributing significantly more to deforestation than smallholders.

Finally, we examine heterogeneity by initial forest cover. Deforestation responds most strongly to palm oil prices in cells with moderate initial cover (Figure 3C). Cells with low forest cover show limited response, as little land remains available for expansion. Conversely, cells with high forest cover—typically in remote and harder-to-access regions—also exhibit smaller responses, likely due to higher clearing costs. This pattern implies that while palm expansion during the study period occurred predominantly in natural forests, it had not yet fully penetrated the most densely forested areas.

Because oil palm is a perennial crop with a typical 25-year replanting cycle, growers may consider not only the recent price change as the baseline model specifies, but also persistent price changes. To explore these dynamics, we estimate deforestation responses to revenues constructed from prices over longer periods. Figure 3D shows that the cumulative effect remains similar to the baseline model, which includes only a one-year lag. Supplementary Information Section D reports similar results over different lag structures, and that the deviation of last year's price from the past five-, seven-, or ten-year average significnatly affects deforestation. These results show that farmers place greater weight on recent price changes when making deforestation decisions, further supporting the baseline specification.

To compare results from the long-run palm supply elasticity model (Figure 2B) with those from the deforestation-response model, we implement an alternative approach in Supplementary Information Section E. In this approach, we substitute the supply elasticity estimate with the deforestation-response estimate in Figure 3A. This method also more explicitly accounts for cumulative supply effects from past expansions, recognizing that oil palm is a perennial crop. The alternative estimate—a 20.7% price increase—closely aligns with the baseline estimate of 20.8%, reinforcing the robustness of our findings.

Deforestation emissions exceed those from fossil diesel

Based on the estimated impact of palm oil prices on deforestation, we estimate that the palm oil price increases driven by global BBD use from 2002 to 2018 led to an additional 1.7 Mha of forest-to-palm conversion in Indonesia and Malaysia (90% confidence interval: [1 Mha, 2.3 Mha]) compared to the BAU scenario. This accounts for roughly 20% of the total forest-to-palm conversion in Indonesia and Malaysia over this period. The total net BBD-driven carbon emissions from land-use change amount to approximately 1074.5 Tg CO2e (Table 1 column 1), or an ILUC carbon intensity (CI) of 83.2g CO2e per megajoule (MJ) of BBD (Table 1 column 4) (90% confidence interval: [48.6 g CO2e/MJ, 112.9 g CO2e/MJ]).

We only consider emissions associated with induced land-use change. Including other lifecycle stages, such as cultivation, fertilizer use, processing, transport, and distribution, increases the full carbon footprint. Government estimates suggest that these additional stages contribute 34.6–63.5 g CO_2e/MJ for palm BBD in the EU and US (13; 14). Adding these quantities to our estimate implies life cycle emissions of at least 117.8–146.7 g CO_2e/MJ. Moreover, our estimates exclude potential carbon emissions from BBD-driven expansion of other vegetable oils and additional palm oil production outside Indonesia and Malaysia, suggesting that they provide a conservative lower bound on the land-use change effects of BBD use.

For comparison, the emissions of petroleum diesel are about 97 g CO_2e/MJ. This total includes combustion emissions of about 75.25 g CO_2e/MJ and refining and production emissions of 21.75 g CO_2e/MJ, based on US EPA estimates (12; 13). Thus, even without considering emissions from land use change outside Malaysia and Indonesia, the CI of palm-based BBD exceeds that of petroleum diesel. These results imply that when land-use change is considered, BBD usage from 2002-2018 increased, rather than reduced, emissions relative to petroleum diesel fuel.

To understand where these emissions come from, we decompose total land-use change emissions into their underlying carbon sources. Land ecosystems store large amounts of carbon both above and below ground. Clearing land for palm production releases this carbon. We estimate that biomass loss—including above-ground biomass (AGB) and below-ground biomass (BGB)—from BBD-induced conversion released approximately 749.4 Tg CO_2e (Table 1 column 1).

Peatland degradation constitutes another major source of emissions. Tropical peat swamp forests form massive carbon sinks, with an estimated deposit of 69 Gt of carbon in Southeast Asia (32). Indonesia and Malaysia together hold the world's largest share of tropical peat carbon, contributing about 74% and 60% of the total forest soil carbon pool in each country, respectively (33). Plantation development on peatland leads to decomposition and continuous carbon release. Using palm plantation maps (22), initial forest type data (23), and peatland maps (25), we estimate that between 2002 and 2018, about 8% of palm plantations expanded into intact peatland forests and 15% into peatlands already subject to human activity. BBD-driven expansion in these areas contributed about 607.2 Tg CO_2e over a 25-year palm lifecycle.

Palm expansion on non-peat soils also releases soil organic carbon (SOC). Accounting for the extent of non-peat expansion induced by BBD, the associated SOC emissions are estimated at 93.8 Tg CO_2e. At the same time, oil palm trees sequester carbon over their lifecycle. We estimate that plantations established due to BBD expansion will sequester about 376 Tg CO_2e over a 25-year lifespan. Combining these factors, the total net BBD-driven carbon emissions from land-use change amount is 1074.5 Tg CO_2e, which corresponds to an average of 25.1 Mg CO_2e per hectare per year (Table 1 column 2).

Supplementary Information Section F compares our estimates of land-use change emissions with those from other studies. Our results are close to studies that explicitly account

Component	(1) Total emissions (Tg CO_2e)			(2) Per ha per year (Mg CO_2e/ha/yr)	(3) Direct CI (g CO_2e/MJ)	(4) ILUC CI (g CO_2e/MJ)		
	Estimate	90% Interval		Estimate	Estimate	Estimate	90% Interval	
		upper	lower				upper	lower
Biomass carbon (AGB+BGB)	749.4	437.9	1016.8	17.5	160.8	58.0	33.9	78.7
Non-peat soil organic carbon	93.8	54.8	127.3	2.2	20.1	7.3	4.2	9.9
Peat decomposition	607.2	354.8	823.9	14.2	130.3	47.0	27.5	63.8
Carbon sequestered by oil palm	-376.0	-219.7	-510.1	-8.8	-80.7	-29.1	-17.0	-39.5
Net carbon emissions from ILUC	1074.5	627.8	1457.8	25.1	230.6	83.2	48.6	112.9

Table 1: Carbon emissions from land-use change due to oil palm expansion. Total emissions are amortized over 25 years to calculate emissions per hectare per year and carbon intensity (CI), consistent with the typical oil palm replanting cycle. This amortization period aligns with international policy conventions, falling between the U.S. EPA's 30-year standard and the EU's 20-year standard.

for emissions at the exact deforestation locations, while they diverge more from studies that apply uniform biomass values across broad forest categories without considering variation by initial forest type or geography. This reinforces the importance of identifying the locations of forest-to-palm conversion and accounting for heterogeneity, as the environmental impacts and carbon emissions of converting different forest types and regions into feedstock plantations vary substantially.

Forest-to-palm conversion for BBD production yields a direct CI of 230.6 g CO_2e/MJ (Table 1, Column 3), calculated as the ratio of net carbon emissions to the palm-based BBD volume produced from the converted area. However, only a portion of global BBD is derived from palm oil—about 35% of the vegetable oils used in BBD in 2018. Large amounts are produced from other vegetable oils, which we have shown are highly substitutable with palm oil. Markets allocate vegetable oils to BBD production through price increases that incentivize production of all oils, including palm, and through reductions in demand by other users.

To translate deforestation emissions into indirect land-use change CI per unit of energy driven by BBD demand, we divide induced net carbon emissions by the amount of BBD energy produced from vegetable oils in 2002-2018. We obtain a CI of 83.2 g CO_2e/MJ (90%

confidence interval: [48.6, 112.9], Table 1 column 4), which represents the forest-to-palm emissions attributable to the MJ of BBD demand during the study period. This estimate excludes potential carbon emissions from BBD-induced expansion of other vegetable oils and palm oil production outside Indonesia and Malaysia, so it provides a lower bound on the land use change effects of BBD use. Moreover, this approach does not account for welfare losses borne by consumers from higher vegetable oil prices.

Conclusion and discussion

Biofuels have become an important weapon in the world's attempts to decarbonize transportation, and biomass-based diesel fuels play an increasing role in the fuel supplies in many countries. However, after taking land use change into account some biofuels may have higher carbon emissions than the fossil fuels they replace. Most work on biofuel-driven land use change to date has focused on the use of corn as a feedstock for the production of ethanol (1; 4; 2). This study focuses on land use changes related to the production of BBD and, specifically, in Indonesia and Malaysia, from the conversion of forest lands into palm plantations. Conversion of these lands for biofuel production is regarded as particularly harmful in terms of carbon emissions, as well as for the loss of biodiversity and other environmental benefits provided by these forests.

Our findings imply that BBD use, rather than delivering climate benefits, likely increases net carbon emissions. These calculations do not incorporate biodiversity losses, which are particularly severe in tropical forests (34; 35), suggesting the true environmental costs are likely greater. Moreover, during our study period, palm expansion had not yet penetrated the most remote and densely forested areas, which generally hold higher carbon stocks. Continued expansion into such areas would further amplify carbon emissions. Such expansion appears likely as governments continue to expand BBD requirements and as they begin to incentivize sustainable aviation fuel, which can be produced using similar processes to BBD.

Policies in some countries, such as the EU and the US, recognize the harms associated with the use of palm oil in bio-based diesel fuel production and seek to curtail its use. However, such policies are unlikely to effectively mitigate deforestation in Indonesia and Malaysia. Because of the high substitutability across vegetable oils, restrictions on palm oil simply shift demand to other oils, which then raise palm prices indirectly as it substitutes for the displaced oils in cooking. More effective mitigation may come from expanding the role of alternative feedstocks, such as tallow and used cooking oil, in BBD production because these feedstocks likely do not cause significant adverse land use change effects.

References

[1] Searchinger, T. *et al.* Use of U.S. croplands for biofuels increases greenhouse gases through emissions from land-use change. *Science* **319**, 1238–1240 (2008). https://www.science.org/doi/pdf/10.1126/science.1151861.

[2] Lark, T. J. *et al.* Environmental outcomes of the US renewable fuel standard. *PNAS* **119** (2022).

[3] Searchinger, T., Peng, L., Zionts, J. & Waite, R. The global land squeeze: Managing the growing competition for land. Tech. Rep., World Resources Institute, Washington, D.C. (2023). URL https://doi.org/10.46830/wrirpt.20.00042.

[4] Lustgarten, A. Palm Oil Was Supposed to Help Save the Planet. Instead It Unleashed a Catastrophe. *The New York Times* (2018). https://www.nytimes.com/2018/11/20/magazine/palm-oil-borneo-climate-catastrophe.html.

[5] Austin, K. G., Schwantes, A., Gu, Y. & Kasibhatla, P. S. What causes de-

forestation in Indonesia? *Environmental Research Letters* **14**, 024007 (2019). https://dx.doi.org/10.1088/1748-9326/aaf6db.

[6] Gaveau, D. L. A. *et al.* Slowing deforestation in Indonesia follows declining oil palm expansion and lower oil prices. *PLOS ONE* **17**, e0266178 (2022). https://journals.plos.org/plosone/article?id=10.1371/journal.pone.0266178.

[7] Gaveau, D. L. *et al.* Rise and fall of forest loss and industrial plantations in Borneo (2000–2017). *Conservation Letters* **12**, e12622 (2019). https://onlinelibrary.wiley.com/doi/abs/10.1111/conl.12622.

[8] Hashempour-Baltork, F., Torbati, M., Azadmard-Damirchi, S. & Savage, G. P. Vegetable oil blending: A review of physicochemical, nutritional and health effects. *Trends in Food Science & Technology* **57**, 52–58 (2016). https://www.sciencedirect.com/science/article/pii/S0924224416302886.

[9] Hinrichsen, N. Commercially available alternatives to palm oil. *Lipid Technology* **28**, 65–67 (2016). https://www.ncbi.nlm.nih.gov/pmc/articles/PMC4834613/.

[10] Declerck, F., Hikouatcha, P., Tchoffo, G. & Tédongap, R. Biofuel policies and their ripple effects: An analysis of vegetable oil price dynamics and global consumer responses. *Energy Economics* **128**, 107127 (2023). https://www.sciencedirect.com/science/article/pii/S0140988323006254.

[11] Yu, Q. *et al.* A cultivated planet in 2010 – part 2: The global gridded agricultural-production maps. *Earth System Science Data* **12**, 3545–3572 (2020). https://essd.copernicus.org/articles/12/3545/2020/.

[12] US Environmental Protection Agency. Greenhouse gas equivalencies calculator - calculations and references. https://www.epa.gov/energy/greenhouse-gas-equivalencies-calculator-calculations-and-references. Accessed at 7/5/2025.

[13] US Environmental Protection Agency. Lifecycle greenhouse gas emissions for select pathways. https://www.epa.gov/sites/default/files/2016-07/documents/select-ghg-results-table-v1.pdf (2016). Accessed at 7/5/2025.

[14] European Union. Directive (EU) 2018/2001 of the European Parliament and of the Council of 11 December 2018 on the promotion of the use of energy from renewable sources. https://eur-lex.europa.eu/eli/dir/2018/2001/oj/eng (2018). Accessed at 7/5/2025.

[15] Broch, A., Hoekman, S. K. & Unnasch, S. A review of variability in indirect land use change assessment and modeling in biofuel policy. *Environmental Science & Policy* **29**, 147–157 (2013). https://www.sciencedirect.com/science/article/pii/S1462901113000208.

[16] Warner, E., Zhang, Y., Inman, D. & Heath, G. Challenges in the estimation of greenhouse gas emissions from biofuel-induced global land-use change. *Biofuels, Bioproducts and Biorefining* **8**, 114–125 (2014). https://scijournals.onlinelibrary.wiley.com/doi/pdf/10.1002/bbb.1434.

[17] Cui, J. & Martin, J. I. Impacts of US biodiesel mandates on world vegetable oil markets. *Energy Economics* **65**, 148–160 (2017). https://www.sciencedirect.com/science/article/pii/S0140988317301172.

[18] Taheripour, F. & Tyner, W. E. US biofuel production and policy: implications for land use changes in Malaysia and Indonesia. *Biotechnology for Biofuels* **13**, 11 (2020). https://doi.org/10.1186/s13068-020-1650-1.

[19] Daioglou, V. *et al.* Progress and barriers in understanding and preventing indirect land-use change. *Biofuels, Bioproducts and Biorefining* **14**, 924–934 (2020). https://scijournals.onlinelibrary.wiley.com/doi/pdf/10.1002/bbb.2124.

[20] Berry, S., Searchinger, T. & Yang, A. Biofuels, deforestation, and the GTAP model. *Tobin Center Working Paper Series* (2024).

[21] Hansen, M. C. *et al.* High-resolution global maps of 21st-century forest cover change. *Science* **342**, 850–853 (2013). https://www.science.org/doi/pdf/10.1126/science.1244693.

[22] Descals, A., Gaveau, D. L. A., Wich, S., Szantoi, Z. & Meijaard, E. Global mapping of oil palm planting year from 1990 to 2021. *Earth System Science Data* **16**, 5111–5129 (2024). https://essd.copernicus.org/articles/16/5111/2024/.

[23] Xu, H. *et al.* Changes in the fine composition of global forests from 2001 to 2020. *Journal of Remote Sensing* **4**, 0119 (2024). https://spj.science.org/doi/pdf/10.34133/remotesensing.0119.

[24] Harris, N. L. *et al.* Global maps of twenty-first century forest carbon fluxes. *Nature Climate Change* **11**, 234–240 (2021). URL https://doi.org/10.1038/s41558-020-00976-6.

[25] Global Forest Watch. Global peatlands. https://data.globalforestwatch.org/datasets/gfw::
peatlands/about. Accessed at 03/31/2025.

[26] US Energy Information Administration. Monthly biofuels capacity and feedstocks update. https://www.eia.gov/biofuels/update/ (2025). Accessed at 09/01/2025.

[27] Rum, I. A., Tukker, A., de Koning, A. & Yusuf, A. Impact assessment of the EU import ban on Indonesian palm oil: Using environmental extended multi-scale mrio. *Science of The Total Environment* **853**, 158695 (2022). https://www.sciencedirect.com/science/article/pii/S0048969722057941.

[28] Feintrenie, L., Chong, W. K. & Levang, P. Why do farmers prefer oil palm? lessons learnt from Bungo District, Indonesia. *Small-scale Forestry* **9**, 379–396 (2010).

[29] Woittiez, L. S., van Wijk, M. T., Slingerland, M., van Noordwijk, M. & Giller, K. E. Yield gaps in oil palm: A quantitative review of contributing factors. *European Journal of Agronomy* **83**, 57–77 (2017). https://www.sciencedirect.com/science/article/pii/S1161030116302131.

[30] Malins, C., Plevin, R. & Edwards, R. How robust are reductions in modeled estimates from GTAP-BIO of the indirect land use change induced by conventional biofuels? *Journal of Cleaner Production* **258**, 120716 (2020). https://www.sciencedirect.com/science/article/pii/S0959652620307630.

[31] Descals, A. *et al.* High-resolution global map of smallholder and industrial closed-canopy oil palm plantations. *Earth System Science Data* **13**, 1211–1231 (2021). https://essd.copernicus.org/articles/13/1211/2021/.

[32] Miettinen, J., Shi, C. & Liew, S. C. Land cover distribution in the peatlands of Peninsular Malaysia, umatra and Borneo in 2015 with changes since 1990. *Global Ecology and Conservation* **6**, 67–78 (2016). https://www.sciencedirect.com/science/article/pii/S2351989415300470.

[33] Page, S. E., Rieley, J. O. & Banks, C. J. Global and regional importance of the tropical peatland carbon pool. *Global Change Biology* **17**, 798–818 (2011). https://onlinelibrary.wiley.com/doi/abs/10.1111/j.1365-2486.2010.02279.x.

[34] Barlow, J. *et al.* Anthropogenic disturbance in tropical forests can double biodiversity loss from deforestation. *Nature* **535**, 144–147 (2016). URL https://doi.org/10.1038/nature18326.

[35] Tudge, S. J., Purvis, A. & Palma, A. D. The impacts of biofuel crops on local biodiversity: a global synthesis. *Biodiversity and Conservation* **30**, 2863–2883 (2021). URL https://doi.org/10.1007/s10531-021-02232-5.

[36] Bronfenbrenner, M. Notes on the elasticity of derived demand. *Oxford Economic Papers* **13**, 254–261 (1961). URL `http://www.jstor.org/stable/2662028`.

[37] James Seale, J., Regmi, A. & Bernstein, J. International evidence on food consumption patterns. Technical Bulletin 1904, U.S. Department of Agriculture, Economic Research Service (2003). URL `https://www.ers.usda.gov/sites/default/files/`$_{l}aserfiche/publications/$47429/14755$_{t}b$1904
83206.*Accessed*10/24/2025.

[38] Engle, R. F. & Granger, C. W. J. Co-integration and error correction: Representation, estimation, and testing. *Econometrica* **55**, 251–276 (1987). `http://www.jstor.org/stable/1913236`.

[39] CME Group. Spread trading in CBOT soybean oil and bmd crude palm oil (2017). Accessed at 08/05/2025, `https://www.cmegroup.com/trading/agricultural/files/spreading-cbot-soybean-oil-and-bmd-crude-palm-oil.pdf`.

[40] Noojipady, P. *et al.* Managing fire risk during drought: the influence of certification and El Niño on fire-driven forest conversion for oil palm in Southeast Asia. *Earth System Dynamics* **8**, 749–771 (2017). `https://esd.copernicus.org/articles/8/749/2017/`.

[41] Cisneros, E., Kis-Katos, K. & Nuryartono, N. Palm oil and the politics of deforestation in Indonesia. *Journal of Environmental Economics and Management* **108**, 102453 (2021). `https://www.sciencedirect.com/science/article/pii/S009506962100036X`.

[42] Busch, J. *et al.* Reductions in emissions from deforestation from Indonesia's moratorium on new oil palm, timber, and logging concessions. *Proceedings of the National Academy of Sciences* **112**, 1328–1333 (2015). `https://www.pnas.org/doi/pdf/10.1073/pnas.1412514112`.

[43] Groom, B., Palmer, C. & Sileci, L. Carbon emissions reductions from Indonesia's moratorium on forest concessions are cost-effective yet contribute little to Paris pledges. *Proceedings of the National Academy of Sciences* **119**, e2102613119 (2022). https://www.pnas.org/doi/abs/10.1073/pnas.2102613119.

[44] Carlson, K. M. *et al.* Carbon emissions from forest conversion by kalimantan oil palm plantations. *Nature Climate Change* **3**, 283–287 (2013). URL https://doi.org/10.1038/nclimate1702.

[45] Guillaume, T. *et al.* Carbon costs and benefits of Indonesian rainforest conversion to plantations. *Nature Communications* **9**, 2388 (2018). URL https://doi.org/10.1038/s41467-018-04755-y.

[46] Roberts, M. J. & Schlenker, W. Identifying supply and demand elasticities of agricultural commodities: Implications for the US ethanol mandate. *American Economic Review* **103**, 2265–95 (2013). https://www.aeaweb.org/articles?id=10.1257/aer.103.6.2265.

[47] Hendricks, N. P., Janzen, J. P. & Smith, A. Futures prices in supply analysis: Are instrumental variables necessary? *American Journal of Agricultural Economics* **97**, 22–39 (2015). https://onlinelibrary.wiley.com/doi/pdf/10.1093/ajae/aau062.

Methods

We estimate the impacts of global BBD use on deforestation in Indonesia and Malaysia and the corresponding carbon emissions by linking a series of empirical models. First, we assess the impact of BBD use on palm oil prices by modeling global supply and demand for palm and cooking oils more generally. Second, we estimate the effect of palm oil prices on deforestation, leveraging observed remote sensing data and panel econometric techniques. Lastly, we combine these estimates to quantify the effect of BBD consumption on deforestation outcomes and carbon emissions.

This empirical strategy offers several advantages and contributions. First, it provides direct evidence on the environmental impacts of biofuel policies based on observed prices and land-use outcomes, minimizing assumptions and reliance on prescribed parameters. Second, it allows us to examine heterogeneity in price effects across regions in Indonesia and Malaysia with different environmental values. Third, by using high-resolution remote sensing data to detect the actual location of forest-to-palm conversion, we avoid reliance on assumptions about land types and enable the inclusion of unmanaged land, which is typically excluded from CGE models investigating ILUC (20). Remote sensing data also help overcome the limitations of government statistics that often under report deforestation (49; 41). Fourth, we empirically model supply and demand for palm and cooking oils, offering evidence on both the high substitutability among cooking oils and the limited role of intensive-margin responses (yield increases) in offsetting demand shocks. The following subsections describe the methodologies and data used in each step.

Effects of BBD on palm oil prices

To evaluate the effects of BBD consumption on palm oil prices, we construct exogenous yield shocks (46) using production data from the FAO from 1961 to 2022 to estimate aggregated demand flexibilities for the four major oil crops and supply elasticities for the three oil crops besides oil palm. For oil palm supply, we rely on data from 1976 to 2019 from the USDA Foreign Agricultural Service (FAS) due to inconsistencies in FAO's reporting of harvested versus planted area for perennial crops. We obtain price data from the World Bank.

For the demand side, we estimate an inverse demand function for palm oil using two-stage least squares (46) as follows:

First stage:

$$q_t = \xi_0 + \xi_1 \omega_t + h_1(t) + v_t. \tag{1}$$

Second stage:

$$P_t^{po} = \beta_0 + \beta_1 Q_t + h_2(t) + \epsilon_t, \tag{2}$$

Here P^{po} is the log price of palm oil and Q represents the log production of various oil crops. Depending on the model specification, Q represents palm fruit, the aggregate of the three major annual oil crops (soybeans, rapeseed, and sunflower), or the aggregate of all four crops (the three plus palm fruit). We use the December price because the production during the year affects the price at the end of the year. The parameter β_1 equals the price flexibility of demand, which is the reciprocal of demand elasticity ($\epsilon^D = \frac{1}{\beta_1}$). The regressions include flexible time trends, $h_1(t)$ and $h_2(t)$ to allow intercepts to evolve over time. The baseline model specifies these trends using restricted cubic splines with five knots. Given that production and price are mutually determined, we follow previous studies and use yield shocks (ω) as an instrumental variable for production to address the endogeneity of Q to demand shocks (46; 47).

Yield shocks are the log average deviations of yields from crop- and country-specific yield trends across production countries, weighted by predicted yield and growing area (47). The underlying yield trends are estimated using restricted cubic splines with five knots. The yield shocks are primarily caused by random weather events. Supplementary Information Section G, provides details on the construction of yield shocks and their validity as an instrument, and Supplementary Information Section H presents sensitivity checks on the derivation of yield shocks.

We estimate the oil supply elasticity separately for oil palm, which is a perennial crop, and the other three major oil crops, which are annuals. The supply equation is:

$$q_t = \alpha_0 + \sum_{s=1}^{k} \alpha_s P_{t-s}^{po} + \delta\omega_t + g(t) + \varepsilon_t, \tag{3}$$

where q_t is the log production of palm fruit or the three major annual oil crops (soybeans, rapeseed, and sunflower), depending on the model specification. The term, $g(t)$, is a flexible time trend. The estimate α_s represents the price elasticity of supply at lag s. Following previous literature (47), the model controls for realized yield shocks (ω) as a proxy for expected shocks. Since markets for storable goods incorporate production expectations, prices can become endogenous to supply. Controlling for yield shocks helps address this endogeneity by accounting for partially predictable production variations. Consistent with empirical evidence that farmers form price expectations based on recent prices (53), we use the lagged annual average palm oil prices for P.

For the short-run supply, we include only one lag ($k = 1$). For the long run, we allow multiple lags and evaluate the cumulative elasticity because producers may respond to price changes gradually over time, especially for oil palm (Supplementary Information Section C provides more details about lag length selection). The aggregated supply elasticity is then calculated as a weighted average of the two elasticities, given by $\epsilon^S = \epsilon^{Sp} s^p + \epsilon^{So} s^o$, where ϵ^{Sp} and ϵ^{So} are the supply elasticities of palm oil and the other three oil crops, respectively; s^p is the market share of palm oil among the main vegetable oils, and s^o is the combined share of the other three oils.

Finally, to link these elasticity estimates to the effects of BBD on palm oil prices, we use OECD data on vegetable oil used for BBD. From 2002 to 2018, global BBD use accounted for approximately 8.5% of the combined global production of palm, soybean, canola, and sunflower oils. Using the demand and supply elasticities estimated above, we calculate the effect of BBD consumption on palm oil prices. A demand shift of percentage $\Delta\%Q$ changes the equilibrium price by $\Delta\%P = \frac{\Delta\%Q}{\epsilon^S - \epsilon^D}$. We use this relationship and calculate the business-as-usual price in the absence of BBD demand.

We further consider two potential sources of bias in our estimates. First, our analysis focuses on the effects of BBD between 2002 and 2018, but the demand and supply elasticities are estimated using a longer time series extending further back. A potential concern is that market behavior in earlier decades may differ from recent years—particularly as BBD demand became more persistent—so elasticities estimated from older data may not fully reflect current responsiveness. To address this concern, we included a post-2000 dummy in both the demand and supply models. The results show no significant differences in elasticities before and after 2000 (Supplementary Information Section A), suggesting that our elasticity estimates are stable over time and not biased by the inclusion of earlier years.

Second, the OECD reports global BBD feedstock use only at the aggregate vegetable oil level—including the four major oils analyzed here (palm, soybean, rapeseed, and sunflower) as well as smaller contributors such as coconut, cottonseed, and groundnut oils. These major oils account for roughly 90% of global vegetable oil production, while the remainder contribute negligibly to BBD output. Therefore, our assumption that 8.5% of total vegetable oil use was devoted to BBD during 2002–2018 is conservative, and the true share is likely higher.

Effect of palm price on deforestation

To estimate the impact of palm oil prices on deforestation in Indonesia and Malaysia, we constructed a panel dataset covering 32,305 grid cells (9 km × 9 km) from 2002 to 2018. The main outcome of interest is the deforestation area converted to oil palm. We combine the Global Forest Change (GFC) dataset (21), oil palm planting-year maps (22), and a pre-clearing vegetation map (23) to identify this variable. GFC is one of the most widely used datasets on forest loss (57), providing a 2000 baseline forest map at 30-meter resolution. Following Indonesia's official definition, we classify as forest any area with canopy cover greater than 30%. By merging GFC with planting-year maps (10 m resolution), we identify annual forest-to-palm conversion.

A challenge is that GFC defines all vegetation taller than 5 meters as forest, including planted forests, agroforests, and oil palm plantations. Since these land types differ substantially in ecological value (58), and replanting palm does not constitute deforestation, we use the 2001 pre-clearing vegetation map (100 m resolution) to distinguish natural forest from planted forest and exclude palm-to-palm replanting from our deforestation measure. The palm planting-year map provides establishment dates until 2021, but very young plantations established in the final years are under detected, as they are not yet visible in the satellite imagery. To address this, we exclude the last three years of data. Our analysis thus focuses on 2002–2018.

To construct annual, cell-specific attainable revenue from palm production, we incorporated oil palm attainable yields from UN FAO's GAEZ dataset (https://gaez.fao.org/) and World Bank price data. The resolution of the GAEZ dataset is 5 arc minutes (about 9 km at the equator). We also used ERA-Interim weather data (59) to control for confounding factors.

We estimated the following empirical model to investigate the price effects on deforestation in Indonesia and Malaysia:

$$dp_{ct} = \alpha_0 + \theta R_{c,t-1} + \alpha_c + \tau_{st} + \epsilon_{ct}, \tag{4}$$

where dp_{ct} represents the area of deforestation for palm plantations in cell c year t and R_{ct} is the attainable revenue from palm oil production. This revenue is calculated as the product of the international price P_t and attainable yields (a_c) for each cell, expressed as $R_{ct} = P_t \times a_c$. Regressions include cell fixed effects α_c to account for all time-invariant characteristics of each cell. The preferred specifications incorporate country-year fixed effects (τ_{st}) to capture national policy changes or other country-specific shocks that could promote or hinder deforestation in the country s year t. We also examine different time controls, including year fixed effects and a time trend that varies by initial cover to capture heterogeneous deforestation pressures. Standard errors are clustered at the second-level administrative unit, reflecting the role of local governments in granting permits for palm expansion and logging (60; 41).

In the baseline, we regress deforestation on attainable revenue lagged one year, capturing responses to recent price changes. Since oil palm is a perennial crop with long investment horizons, we also test alternative revenue specifications, including longer lags, multi-year averages, and deviations from long-term price trends. To assess robustness, we examine reverse causality (i.e., whether expectations of future palm expansion affect current prices), additional weather controls, and sensitivity to attainable yield definitions (Supplementary Information, Section D).

Effects of BBD use on carbon emissions

We calculate carbon emissions by quantifying changes in carbon stocks resulting from forest-to-oil palm conversion between 2002 and 2018. The accounting includes emissions from above-ground biomass (AGB), below-ground biomass (BGB), soil organic carbon (SOC) in non-peatland, and peatland decomposition, net of the carbon sequestered by oil palm trees. In Supplementary Information Section F, we assess the robustness of our carbon emission estimates from land-use change by comparing them with findings from previous studies conducted in similar regions.

For biomass-related emissions, we estimate the biomass of deforested areas using the Aboveground Live Woody Biomass Density Map (24) and apply a below-to-above-ground biomass ratio of 0.24 (42). AGB and BGB are then converted to carbon stocks using a biomass-to-carbon ratio of 0.47 (24).

To capture emissions from peatlands, we combine the peatland map (25), the palm plantation map (31), and the pre-clearing vegetation map (23) to identify palm expansion into peatland across different initial forest types. For conversion of disturbed peatland forests (natural forests with management, planted forests, and agroforestry), we adopt the IPCC estimate of 40 Mg CO_2e ha^{-1} yr^{-1} for long-term drained organic peat soils (65), which excludes the initial emission peak. For conversion of intact peatland forests, we use an average of 100 Mg CO_2e ha^{-1} yr^{-1} over 25 years (66).

Emissions from SOC in non-peat areas and carbon sequestration by oil palm trees are based on (67). All biomass and non-peat soil emissions are amortized over 25 years, consistent with the typical oil palm replanting cycle. This amortization period is aligned with international policy conventions, falling between the U.S. EPA's 30-year and the EU's 20-year standards. We estimate that about 20% of the total forest-to-palm conversion during 2002-2018 is due to BBD demand, and proportionally assign the corresponding land-use change emissions to BBD.

To derive the carbon intensity of BBD per unit of energy, we use the biodiesel conversion rate of crude palm oil and energy content data from USDA (68). Since BBD includes both biodiesel (BD) and renewable diesel (RD), we rely on BD's conversion rates, as BD has dominated global BBD production (69). Because RD conversion rates are lower (70), our CI estimates are likely conservative, meaning the true carbon intensity per MJ may be larger than our estimate. We compute confidence intervals using the bootstrap procedure detailed in Supplementary Information Section I.

Data and code availability

All data are publicly available as described in the methods section. Code is available from the authors upon request.

Acknowledgments

This research was supported by the Giannini Foundation for Agricultural Economics. We thank participants in the UC Davis Agricultural Economics seminar and the UC Energy Institute Research Briefing for comments.

Author Contributions

T.J. Chen, R.J. Sexton and A. Smith developed the research methods jointly. T.J. Chen collected the data and conducted the econometric analysis with input from R.J. Sexton and

A. Smith. T.J. Chen wrote the first draft of the manuscript. T.J. Chen, R.J. Sexton and A. Smith edited the manuscript jointly.

Competing interests

The authors declare no competing interests.

Methods References

[48] Berry, S., Searchinger, T. & Yang, A. Biofuels, deforestation, and the GTAP model. *Tobin Center Working Paper Series* (2024).

[49] Burgess, R., Hansen, M., Olken, B. A., Potapov, P. & Sieber, S. The political economy of deforestation in the tropics. *The Quarterly Journal of Economics* **127**, 1707–1754 (2012). URL https://doi.org/10.1093/qje/qjs034. https://academic.oup.com/qje/article-pdf/127/4/1707/30624701/qjs034.pdf.

[50] Cisneros, E., Kis-Katos, K. & Nuryartono, N. Palm oil and the politics of deforestation in Indonesia. *Journal of Environmental Economics and Management* **108**, 102453 (2021). https://www.sciencedirect.com/science/article/pii/S009506962100036X.

[51] Roberts, M. J. & Schlenker, W. Identifying supply and demand elasticities of agricultural commodities: Implications for the US ethanol mandate. *American Economic Review* **103**, 2265–95 (2013). https://www.aeaweb.org/articles?id=10.1257/aer.103.6.2265.

[52] Hendricks, N. P., Janzen, J. P. & Smith, A. Futures prices in supply analysis: Are instrumental variables necessary? *American Journal of Agricultural Economics* **97**, 22–39 (2015). https://onlinelibrary.wiley.com/doi/pdf/10.1093/ajae/aau062.

[53] Chavas, J.-P. On information and market dynamics: The case of the u.s. beef

market. *Journal of Economic Dynamics and Control* **24**, 833–853 (2000). URL https://www.sciencedirect.com/science/article/pii/S0165188999000275.

[54] Hansen, M. C. *et al.* High-resolution global maps of 21st-century forest cover change. *Science* **342**, 850–853 (2013). https://www.science.org/doi/pdf/10.1126/science.1244693.

[55] Descals, A., Gaveau, D. L. A., Wich, S., Szantoi, Z. & Meijaard, E. Global mapping of oil palm planting year from 1990 to 2021. *Earth System Science Data* **16**, 5111–5129 (2024). https://essd.copernicus.org/articles/16/5111/2024/.

[56] Xu, H. *et al.* Changes in the fine composition of global forests from 2001 to 2020. *Journal of Remote Sensing* **4**, 0119 (2024). https://spj.science.org/doi/pdf/10.34133/remotesensing.0119.

[57] Pendrill, F. *et al.* Disentangling the numbers behind agriculture-driven tropical deforestation. *Science* **377**, eabm9267 (2022). https://www.science.org/doi/abs/10.1126/science.abm9267.

[58] Tropek, R. *et al.* Comment on "high-resolution global maps of 21st-century forest cover change". *Science* **344**, 981–981 (2014). https://www.science.org/doi/abs/10.1126/science.1248753.

[59] Muñoz Sabater, J. ERA5-land monthly averaged data from 1950 to present. Copernicus Climate Change Service (C3S) Climate Data Store (CDS). DOI: 10.24381/cds.68d2bb30 (2019). Accessed at 10/31/2024.

[60] McCarthy, J. F., Gillespie, P. & Zen, Z. Swimming upstream: Local Indonesian production networks in "globalized" palm oil production. *World Development* **40**, 555–569 (2012). https://www.sciencedirect.com/science/article/pii/S0305750X11001872.

[61] Harris, N. L. *et al.* Global maps of twenty-first century forest carbon fluxes. *Nature Climate Change* **11**, 234–240 (2021). URL https://doi.org/10.1038/s41558-020-00976-6.

[62] Busch, J. *et al.* Reductions in emissions from deforestation from Indonesia's moratorium on new oil palm, timber, and logging concessions. *Proceedings of the National Academy of Sciences* **112**, 1328–1333 (2015). https://www.pnas.org/doi/pdf/10.1073/pnas.1412514112.

[63] Global Forest Watch. Global peatlands. https://data.globalforestwatch.org/datasets/gfw::
peatlands/about. Accessed at 03/31/2025.

[64] Descals, A. *et al.* High-resolution global map of smallholder and industrial closed-canopy oil palm plantations. *Earth System Science Data* **13**, 1211–1231 (2021). https://essd.copernicus.org/articles/13/1211/2021/.

[65] Hiraishi, T. *et al.* *2013 Supplement to the 2006 IPCC Guidelines for National Greenhouse Gas Inventories: Wetlands* (IPCC, 2014).

[66] Hooijer, A. *et al.* Subsidence and carbon loss in drained tropical peatlands. *Biogeosciences* **9**, 1053–1071 (2012). https://bg.copernicus.org/articles/9/1053/2012/.

[67] Pendrill, F. *et al.* Agricultural and forestry trade drives large share of tropical deforestation emissions. *Global Environmental Change* **56**, 1–10 (2019). https://www.sciencedirect.com/science/article/pii/S0959378018314365.

[68] USDA. European Union: Biofuels annual. https://www.fas.usda.gov/data/european-union-biofuels-annual-4 (2024). Accessed at 12/09/2024.

[69] S&P Global. Biodiesel and renewable diesel. https://www.spglobal.com/content/dam/spglobal/ci/en/documents/products/pdf/$\mathrm{CI}_0$325

[70] Uusitalo, V. *et al.* Carbon footprint of renewable diesel from palm oil, jatropha oil and rapeseed oil. *Renewable Energy* **69**, 103–113 (2014). https://www.sciencedirect.com/science/article/pii/S0960148114001657.

Supplementary Methods

A Further details on demand and supply elasticity estimates

Table SI1 reports estimates of demand flexibility for aggregate oil crops with respect to palm oil prices. The baseline model (Column 3) adopts the most flexible specification, a restricted cubic spline with five knots, while Columns 1 and 2 use spline trends with three and four knots, respectively. The estimated coefficients are similar across specifications. Asterisks in all regression tables are based on two-sided p-values unless otherwise noted.

The estimated demand elasticity from the baseline model is -0.29, indicating an inelastic response of vegetable oil demand to price changes. This finding is consistent with the relationship that the elasticity of derived demand for an input is inversely related to its share in production (36). Because vegetable oil represents a relatively small share of total input in food production, its demand tends to be inelastic. Our global demand elasticity estimate is also consistent with (37), who report unconditional own-price demand elasticities for oils and fats across 114 countries: -0.158 for high-income, -0.325 for middle-income, and -0.442 for low-income countries.

Table SI2 presents the demand flexibility estimates when oil palm fruit is separated from the three competing oil crops, under alternative time-trend specifications. The results remain stable across specifications.

Table SI3 examines whether market behavior differed between earlier decades and more recent years, particularly after BBD demand became more persistent in the 2000s. The interaction terms between the post-2000 dummy and the estimated supply elasticities and demand flexibility are both economically small and statistically insignificant. This suggests that the elasticities are stable over time and not biased by the inclusion of earlier years in the estimation sample.

B Vegetable oil prices are cointegrated

We test whether palm oil and other vegetable oil prices are cointegrated using the Engle–Granger method (38). The results indicate that these oil prices move together in the long run, consistent with the view that the major vegetable oils are close substitutes.

Theoretically, if products A and B are perfect substitutes, the marginal rate of substitution (MRS) between them is constant:

$$MRS_{A,B} = \frac{P_A}{P_B} = C,$$

where C is a constant and P_A and P_B denote the prices of goods A and B, respectively. In this case, prices move proportionally. In practice, when the price of one oil rises, consumers substitute perfectly towards other oils, increasing their demand and driving up their prices (39).

Using global price data from 1960 to 2024 from the World Bank, Augmented Dickey–Fuller (ADF) tests indicate that all log price series are nonstationary (I(1)) for the four major oil crops, with the null of a unit root rejected only for their first differences (Table SI4).[1] Residuals from regressions of palm oil prices on each competing oil's prices are stationary (Table SI5), confirming cointegration. The estimates in Table SI5 suggest strong long-run co-movement between palm oil and other major oils. The coefficients are close to unity for soybean and canola oil (about 1.04 and 1.01, respectively), and slightly below unity for sunflower oil (about 0.86). These near one-to-one relationships reinforce the view that the oils are close substitutes in consumption and trade, with price shocks in one market transmitting strongly to others.

[1] Canola oil prices are only available from February 2002 onward, and sunflower oil prices are not available before 2002 and are incomplete for that year.

C Further details on long-run supply response estimates

A long-run supply model considers multiple lags and evaluates the cumulative elasticity, as specified in Eq. (3):

$$q_t = \alpha_0 + \sum_{s=1}^{k} \alpha_s P_{t-s}^{po} + \delta\omega_t + g(t) + \varepsilon_t,$$

which can be re-parameterized as:

$$\begin{aligned} q_t &= \alpha_0 + \sum_{s=1}^{k-1} \zeta_s \Delta P_{t-s}^{po} + \zeta_k P_{t-k}^{po} + \delta\omega_t + g(t) + \varepsilon_t \\ &= \alpha_0 + \alpha_1 \Delta P_{t-1}^{po} + (\alpha_1 + \alpha_2)\Delta P_{t-2}^{po} + \cdots + (\alpha_1 + \cdots + \alpha_{k+1})\Delta P_{t-k+1}^{po} + (\alpha_1 + \cdots + \alpha_k) P_{t-k}^{po} \\ &\quad + \delta\omega_t + g(t) + \varepsilon_t, \end{aligned} \tag{5}$$

where the cumulative effects of lagged prices become more transparent. This formulation facilitates identifying the long-run response pattern. Tables SI6 and SI7 report the detailed estimates of long-run supply elasticities using Eq. (5). Based on the Akaike Information Criterion (AIC) and Bayesian Information Criterion (BIC), the long-run analysis includes 6 lags for the three annual oil crops and 7 lags for oil palm.

The results highlight distinct response dynamics between palm and the other oil crops, reflecting their biological and agronomic differences. For soybeans, rapeseed, and sunflower—annual crops—the production response occurs quickly within one year (Table SI6, Columns 1–3). The main adjustment comes from area expansion (Columns 4–6). Under the specification with 5 knots, yield even shows a small negative response in the first two years (Column 9), possibly because expansion pushes cultivation into marginal land with lower productivity. Over longer horizons, yields increase slightly, possibly from investment in productivity improvements, but the dominant adjustment channel remains area expansion.

In contrast, oil palm exhibits a markedly delayed response. Prices have no significant effects on either harvested area or production until three to five years later, which aligns with the biological lag of oil palm maturation (Table SI7). As with the other crops, the main driver of expansion is cropland area (Columns 4–6). Yield responses are even smaller and more sensitive to alternative time-trend specifications (Columns 7–9). This pattern underscores that palm oil supply adjustment is slow, persistent, and heavily dependent on land conversion, rather than yield intensification.

D Price effects on deforestation are robust to alternate specifications

We performed multiple checks to ascertain the robustness of our deforestation results. We first verified that the main findings are not sensitive to alternative FE or time trend specifications, as shown in Table SI8. The baseline estimate with country–year FE in Column 1 is very similar to the estimates in Columns 2–3, which instead control for year FE and initial forest-cover–decile trends. The decile-specific trends capture differences in deforestation likelihood or pressure associated with initial forest cover, which may potentially covary with attainable revenue.

Another potential concern is that the relationship between prices and deforestation might also reflect reverse causality—i.e., traders might anticipate increased palm production, and this drives down prices. This effect is less likely for a perennial like palm fruits, which take 3-5 years to harvest after planting. To further address this potential concern, we excluded the top 10%, 25%, and 50% of production cells to focus on smaller production areas. The results in Figure 3A rows 4-6 and Table SI9 show that the estimates remain consistent, suggesting reverse causality is not a significant issue.

Weather conditions can be another confounder. Weather influences fire risks, impacts palm production (40), and potentially co-varies with palm oil prices. To mitigate this concern, we controlled for temperature and precipitation in the model, specifying deforestation area as a quadratic function of each.[2] Results, as shown in Table SI10 and Figure 3A rows 7-9, indicate a concave relationship between deforestation area and both temperature and precipitation, although the precipitation coefficients are not statistically significant. Importantly, the estimates for palm revenue remain robust after accounting for weather effects.

Moreover, since the revenue variable is constructed using attainable yields (AY), it is

[2] Temperature and precipitation are demeaned.

possible that the estimates are biased by variations that co-vary with yield potential, as yield potential may correlate with other factors influencing deforestation pressure. To address this concern, we included interaction terms between deciles of attainable yields and linear time trends to allow for different deforestation trends by the yields. Additionally, we tested the sensitivity of the results by dropping extreme values. Table SI11 demonstrates that the estimates remain stable across these robustness tests.

Finally, we test whether growers primarily respond to recent prices, as assumed in the baseline model, or to alternative measures of price dynamics. Table SI12 Columns (1)–(5) and Figure 3D show that one-year-lagged prices account for most of the effect. Columns (5)–(8) of Table SI12 use moving averages of prices over different horizons (from $t-1$ to t, $t-3$, and $t-5$), with results indicating that longer averaging windows attenuate the estimated effect. Following the previous study (41), we also construct a variable capturing the deviation of current prices from multi-year historical averages. The hypothesis is that growers adjust deforestation when current profitability diverges sharply from past norms. Table SI13 reports the results, showing significant estimates for the deviation of last year's price from 5-, 7-, and 10-year averages. These estimates reinforce the conclusion that farmers place greater weight on recent price changes.

E Using supply elasticity implied by the deforestation model does not change estimate of price effect

To assess the robustness of the deforestation estimates and compare results from the long-run palm supply elasticity model with those from the deforestation-response model using remote sensing data, we implement an alternative approach in which BAU prices are estimated from deforestation-response coefficients rather than from the palm long-run supply elasticity. This method also explicitly accounts for the cumulative supply effect of past palm expansion, recognizing that oil palm is a perennial crop and that a one-time expansion generates fruit for many years. Accordingly, we compute net BBD demand shocks by subtracting the palm oil production resulting from earlier expansions.

We begin by estimating BAU prices for the first four years of the study period using only the supply elasticities of competing oil crops, assuming no immediate supply response from palm due to its biological lag. These BAU prices are then combined with the estimated deforestation response to palm oil prices to infer the associated palm-driven deforestation area. This area is converted into palm oil production using adjustments for: (i) the share of production from Indonesia and Malaysia, (ii) the proportion of palm expansion occurring in forests, (iii) palm fruit yields of each year, and (iv) average oil content of palm fruits.

From the fifth year onward, we subtract the additional palm oil production from four years earlier (when the corresponding deforestation occurred) from the BBD-induced demand shock to obtain a net demand shock. The BAU price and associated deforestation for that year are then re-estimated. This iterative process continues for all subsequent years, incorporating the cumulative production effects of earlier expansions.

Using this alternative approach, the average price increase over the study period is 20.7%—similar to the baseline estimate obtained from the long-run palm supply elasticity (20.8%). The total estimated deforestation area of 1.799 million hectares is also close to the baseline estimate of 1.717 million hectares, supporting our main findings.

F Comparison to other estimates of carbon emissions from land-use change in Indonesia

To assess the robustness of our carbon emission estimates from land-use change, we compare them with findings from previous studies conducted in similar regions. Table SI14 presents both our estimates and those from the literature. Our results are broadly consistent with studies that explicitly calculate emissions at the exact deforestation locations (42; 43). For example, we estimate carbon emissions from biomass at 438.2 Mg CO_2e/ha, while Groom et al. (2022) (43) report a higher estimate of 570.1 Mg CO_2e/ha. Their higher figure likely reflects their focus on deforestation in primary and peatland forests, which generally store more carbon.

When summing emissions from biomass, SOC, and peatland, our estimate of 848.1 Mg CO_2e/ha is close to the 749.9 Mg CO_2e/ha reported by Busch et al. (2015) (42). The remaining discrepancy may arise because their scope includes deforestation for logging and timber extraction, in addition to palm expansion, and the study period and area.

By contrast, our estimates differ more from studies that apply uniform biomass values across broad forest categories or locations (44; 45). These studies tend to report higher biomass values than ours, likely because their baseline forests are denser than many of the forests in the actual study area.

Taken together, these comparisons reinforce the importance of identifying the locations of forest-to-palm conversion and accounting for heterogeneity. The environmental impacts and carbon emissions from converting forests into feedstock plantations vary considerably depending on forest type and regional conditions.

G Further details on construction of yield shocks as instrumental variables

We adapt the method from previous studies (46; 47) to model demand and supply. The aggregate oil crop quantity in year t is constructed using the oil production share s_c of each crop c:

$$Q_t = \sum_c s_c Q_{ct}.$$

Aggregate oil production can be decomposed as:

$$Q_t = A_t \, Y_t \, \Psi_t,$$

where A_t is the total growing area, Y_t is the average yield trend (weighted by oil share), and Ψ_t is the average yield shock, primarily driven by weather as shown in the latter part of this section.

Total growing area is measured as the sum of country i and crop c areas across all oil crops in the dataset. This variable reflects the extensive margin of production. Mathematically:

$$A_t = \sum_i \sum_c A_{cit}.$$

The yield trend (Y_t) represents the intensive margin, the technological and agronomic improvements in productivity, net of short-run shocks. For each crop c in country i and year t, we fit a restricted cubic spline trend with five knots to the yield series. We construct the annual yield trend as the weighted average of country–crop-specific yield trends, using weights based on area (A_{cit}) and the oil production share of each crop (s_c):

$$Y_t = \frac{\sum_i \sum_c s_c \times A_{cit} \times Y_{cit}}{\sum_i \sum_c A_{cit}}.$$

Yield shocks (Ψ_{cit}) are defined as deviations from the underlying yield trend, primarily reflecting short-run weather conditions. The shock is computed as the proportional deviation of observed yield from its trend value Y_{cit}. To obtain the annual aggregate yield shock, we average these deviations across all countries and crops, weighting by each crop's oil production share (s_c), its growing area (A_{cit}), and its trend yield (Y_{cit}):

$$\Psi_t = \frac{\sum_i \sum_c s_c \times \Psi_{cit} \times A_{cit} \times Y_{cit}}{\sum_i \sum_c A_{cit} \times Y_{cit}},$$

We denote the log quantity, log area, log yield trend, and log yield shocks as q_t, a_t, y_t, and ω_t. Demand flexibilities for the four major oil crops and supply elasticities for the three annual oil crops are estimated using FAO data from 1961–2022 across all producing countries. For oil palm supply, we rely on USDA FAS data from 1976–2019 for Indonesia, Malaysia, Thailand, and the Philippines, which together account for over 86% of global palm oil production. FAS data are preferred due to inconsistencies in FAO's reporting of harvested versus planted area for perennial crops. The underlying assumption is that producer behavior in these four countries reflects global oil palm supply dynamics.

The log yield shock serves as an instrumental variable and must satisfy both relevance and exogeneity conditions. Relevance follows directly from the production identity: yield shocks are deviations from yield trend, a key determinant of production. Empirically, relevance is confirmed by highly significant first-stage regressions with strong F-statistics (Table SI1).

Exogeneity is a more substantive concern. One potential issue is that yield shocks could be endogenous if they are driven by prices. However, several pieces of evidence suggest this is unlikely. First, yield shocks vary substantially across countries even though all countries are exposed to the same global prices, indicating that they are not mechanically determined by price movements. The correlations are uniformly low across crops, suggesting that shocks are largely idiosyncratic to country-specific conditions, such as weather, rather than global price dynamics.[3] Second, while palm oil prices exhibit strong autocorrelation, aggregate yield shocks show little to no persistence over time, which is consistent with shocks being driven by weather-related events rather than market forces. This distinction is further supported by formal tests: Breusch–Godfrey test statistics for the aggregated yield shocks are very low (0.002–0.083 for all four oil crops, 0.261–0.564 for the three competing crops, and 1.42–1.48 for palm oil), all of which fail to reject the null hypothesis of no autocorrelation. By contrast, test statistics for palm oil prices range from 10.7–20.1, exceeding the 1% critical value in all cases, indicating strong autocorrelation. Taken together, this evidence supports the validity of yield shocks as an exogenous instrument.

[3]The correlation coefficients for the top two exporters are −0.118 for soybeans, 0.074 for rapeseed, 0.208 for sunflower seed, and 0.086 for palm based on FAO data, 1961–2022). For palm based on FAS data (1976–2019), the correlation coefficient is 0.291.

H Demand and supply elasticities not sensitive to assumptions in yield shock construction

The baseline model constructs yield shocks using a flexible yield trend based on restricted cubic splines with five knots. To test the sensitivity of the results to the choice of yield shock construction, we re-estimate the demand and supply models using trends with three and four knots. Table SI15 presents results for the demand model, while Tables SI16, SI17, SI18, and SI19 report results for the short-run palm supply model, the short-run supply of the other oil crops, the long-run palm supply model, and the long-run supply of the other crops, respectively.

For each specification of yield shocks derived from a different trend (Row 1), we also vary the flexible time trends that allow intercepts to evolve over time. The baseline includes restricted cubic splines with five knots, while we additionally test specifications with three and four knots, as indicated in the last row of each table. The estimates are robust across all specifications.

I Bootstrap method for computing confidence interval of BBD-induced deforestation

To construct the confidence interval for the deforestation area attributable to BBD policies, we use a bootstrap approach designed to account for potential correlation between elasticity estimates and the nonlinear transformation used in the calculation. The procedure is as follows:

1. We first detrend the dependent and independent variables in the demand and supply equations (Eq. (2) and (3)). To address autocorrelation, we apply a block bootstrap. The detrended observations are divided into the ceiling of n/m blocks of length m, with $m = 2$ as the baseline choice.[4]

2. Because the sample length n differs across the palm supply, other crop supply, and demand models (and in lagged specifications), we oversample blocks and then retain the first n observations. In cases where n/m is not an integer, the position of a year within a block affects its sampling probability (earlier positions are more likely to be selected). To correct for this, we randomly select observations from the last (possibly truncated) block.

3. We then add the original trend back to the detrended bootstrap sample and re-estimate the elasticities or flexibilities. This process is repeated 10,000 times.

4. Separately, we draw 10,000 random values of the estimated price effect on deforestation in Eq. (4), θ, from a normal distribution with the mean and variance obtained from the OLS regression. Given the large sample size in this regression, the normal approximation from asymptotic theory is appropriate. We assume zero covariance between θ and the elasticity estimates, as they are derived from different datasets covering different time periods.

[4] We also test $m = 3$ and obtain similar estimates. Choosing $m > 1$ helps preserve temporal autocorrelation.

5. For each draw, we compute the deforestation effect using Eq. (4). We then obtain a confidence interval by applying the percentile interval method; we use the 5th and 95th percentiles of the distribution to form a 90% confidence interval.[5]

[5]The percentile method is appropriate given that the bootstrap distributions are approximately symmetric. We do not use the percentile-t method because the standard error of the deforestation estimate is not available, given the unclear correlation structure between the elasticity estimates and the nonlinear transformation.

Supplementary Tables

Table SI1: Inverse demand for palm oil with respect to four aggregated oil crops under alternative flexible time trend specifications

	Log palm oil prices		
	(1)	(2)	(3)
Log oil crops q	-2.271*	-2.733**	-3.459***
	(1.286)	(1.172)	(1.062)
First stage			
Shocks ω	1.171***	1.204***	1.190***
	(0.185)	(0.199)	(0.209)
Observations	62	62	62
R-squared	0.497	0.520	0.579
Knots	3	4	5
Effective F	39.95	36.46	32.41

Robust standard errors in parentheses
*** p<0.01, ** p<0.05, * p<0.1

The baseline model (Column 3) uses the most flexible specification, a restricted cubic spline with five knots, while Columns 1 and 2 use spline trends with three and four knots, respectively.

Table SI2: Inverse oil palm demand: separating palm fruit and the three oil crops under alternative flexible time trend specifications

	Log palm oil prices		
	(1)	(2)	(3)
Log palm q	-1.801	-1.797*	-1.898**
	(1.188)	(0.975)	(0.893)
Log three oil crops q	-1.831**	-1.823*	-2.126**
	(0.850)	(0.996)	(0.951)
First stage: Log palm fruit q			
Shock of palm fruit	0.810***	1.063***	1.028***
	(0.275)	(0.219)	(0.145)
Shock of three oil crops	-0.600	-0.319	-0.192
	(0.485)	(0.288)	(0.282)
First stage: Log three oil crops q			
Shock of palm fruit	0.264**	0.218*	0.222*
	(0.128)	(0.121)	(0.122)
Shock of three oil crops	1.250***	1.196***	1.168***
	(0.176)	(0.155)	(0.155)
Observations	62	62	62
R-squared	0.501	0.499	0.528
Knots	3	4	5

Robust standard errors in parentheses
*** p<0.01, ** p<0.05, * p<0.1

The baseline model (Column 3) uses the most flexible specification, a restricted cubic spline with five knots, while Columns 1 and 2 use spline trends with three and four knots, respectively.

Table SI3: Comparison of supply elasticities and demand flexibility across time periods

	Palm supply		Other supply		Demand flexibility	
	Baseline	Cut at 2000	Baseline	Cut at 2000	Baseline	Cut at 2000
	(1)	(2)	(3)	(4)	(5)	(6)
ΔP_{t-1}	0.00516	0.00216	0.0841***	0.0664***		
	(0.0213)	(0.0327)	(0.0228)	(0.0235)		
ΔP_{t-2}	0.0118	0.00404	0.0402	0.0126		
	(0.0158)	(0.0288)	(0.0268)	(0.0290)		
ΔP_{t-3}	0.0315	0.0308	0.0647**	0.0421		
	(0.0220)	(0.0415)	(0.0316)	(0.0391)		
ΔP_{t-4}	0.0150	0.0143	0.0802***	0.0609**		
	(0.0223)	(0.0454)	(0.0212)	(0.0280)		
ΔP_{t-5}	0.0629**	0.0689	0.0843**	0.0894**		
	(0.0275)	(0.0434)	(0.0322)	(0.0395)		
ΔP_{t-6}	0.0485*	0.0626*				
	(0.0257)	(0.0362)				
Log palm oil price P_{t-6}			0.133***	0.134***		
			(0.0282)	(0.0315)		
Log palm oil price P_{t-7}	0.0965***	0.101**				
	(0.0335)	(0.0396)				
$\Delta P_{t-1} \times 1\{Year \geq 2000\}$		0.0260		0.0455		
		(0.0438)		(0.0442)		
$\Delta P_{t-2} \times 1\{Year \geq 2000\}$		0.0283		0.0899**		
		(0.0488)		(0.0416)		
$\Delta P_{t-3} \times 1\{Year \geq 2000\}$		0.0206		0.0390		
		(0.0659)		(0.0457)		
$\Delta P_{t-4} \times 1\{Year \geq 2000\}$		0.0286		0.0689		
		(0.0660)		(0.0457)		
$\Delta P_{t-5} \times 1\{Year \geq 2000\}$		0.00223		-0.0340		
		(0.0446)		(0.0412)		
$\Delta P_{t-6} \times 1\{Year \geq 2000\}$		-0.0234				
		(0.0422)				
Log palm oil price $P_{t-6} \times 1\{Year \geq 2000\}$				0.00151		
				(0.00439)		
Log palm oil price $P_{t-7} \times 1\{Year \geq 2000\}$		-0.00317				
		(0.00390)				
Log oil crops Q					-3.459***	-3.399***
					(1.062)	(0.979)
Log oil crops $Q \times 1\{Year \geq 2000\}$						-0.0563
						(0.0609)
Observations	44	44	57	57	62	62

Robust standard errors in parentheses
*** p<0.01, ** p<0.05, * p<0.1

Columns 1, 3, and 5 present the baseline estimates. Columns 2, 4, and 6 include a post-2000 dummy to test for changes in elasticities over time. The results show no statistically significant differences before and after 2000, indicating stable supply and demand responses.

Table SI4: ADF test statistics for the log price series of major vegetable oils

	Palm oil	Soybean oil	Canola oil	Sunflower oil
Level	-2.109	-1.918	-2.345	-1.834
First difference	-19.906***	-20.258***	-11.363***	-10.782***
Observations	756	756	251	228

The null hypothesis of a unit root is rejected for all first differences of the log price series, indicating stationarity. The ADF test is a one-sided test. Results are similar when using the level price series. The sunflower series begins in 2003 due to gaps in 2002.

Table SI5: Long-run relationships between log palm oil prices and other major vegetable oils

	Soybean oil (1)	Canola oil (2)	Sunflower oil (3)
Log price of a competing oil	1.038***	1.014***	0.862***
	(0.0101)	(0.0317)	(0.0256)
Observations	756	251	228
R-squared	0.933	0.804	0.834
ADF stat. of residuals	-5.991***	-3.482**	-3.530**

The left-hand-side variable is the log price of palm oil. The first row indicates the competing oil considered in the regression. Standard errors in parentheses. The ADF test is a one-sided test. *** $p < 0.01$, ** $p < 0.05$, * $p < 0.1$.

Table SI6: Long-run supply elasticity of the three competing oil crops

	Log quantity (q)			Log area (a)			Log yield (y)		
	(1)	(2)	(3)	(4)	(5)	(6)	(7)	(8)	(9)
ΔP_{t-1}	0.0806***	0.0832***	0.0841***	0.0842***	0.0921***	0.0961***	-0.00367	-0.00887	-0.0120*
	(0.0191)	(0.0185)	(0.0228)	(0.0212)	(0.0198)	(0.0228)	(0.00773)	(0.00659)	(0.00603)
ΔP_{t-2}	0.0391	0.0397	0.0402	0.0450	0.0486*	0.0523*	-0.00586	-0.00894	-0.0121*
	(0.0268)	(0.0256)	(0.0268)	(0.0280)	(0.0264)	(0.0268)	(0.00738)	(0.00726)	(0.00713)
ΔP_{t-3}	0.0635*	0.0637**	0.0647**	0.0624*	0.0673**	0.0743**	0.00114	-0.00360	-0.00962
	(0.0334)	(0.0311)	(0.0316)	(0.0356)	(0.0322)	(0.0312)	(0.0107)	(0.0106)	(0.0102)
ΔP_{t-4}	0.0747***	0.0789***	0.0802***	0.0570***	0.0700***	0.0762***	0.0177*	0.00887	0.00406
	(0.0178)	(0.0152)	(0.0212)	(0.0207)	(0.0183)	(0.0227)	(0.00980)	(0.0113)	(0.0102)
ΔP_{t-5}	0.0797**	0.0829***	0.0843**	0.0649**	0.0762***	0.0827**	0.0147*	0.00665	0.00155
	(0.0307)	(0.0287)	(0.0322)	(0.0300)	(0.0281)	(0.0313)	(0.00778)	(0.00789)	(0.00814)
Log palm oil price P_{t-6}	0.118***	0.130***	0.133***	0.0654***	0.0965***	0.103***	0.0522***	0.0340***	0.0303***
	(0.0212)	(0.0214)	(0.0282)	(0.0214)	(0.0218)	(0.0280)	(0.00603)	(0.0101)	(0.00802)
Shocks ω_t	1.325***	1.316***	1.311***	0.312**	0.288**	0.276**	0.0128	0.0282	0.0359
	(0.129)	(0.128)	(0.130)	(0.125)	(0.120)	(0.122)	(0.0385)	(0.0366)	(0.0402)
Observations	57	57	57	57	57	57	57	57	57
Knots	3	4	5	3	4	5	3	4	5

Long-run supply elasticity of the three competing oil crops (soybeans, rapeseed, and sunflower) with respect to palm oil prices. Model selection criteria for the 7-lag specification of the quantity regression with 5 spline knots are AIC = -216.665 and BIC = -192.577. For comparison, the 7-lag model yields AIC = -215.058 and BIC = -188.963, and the 5-lag model yields AIC = -213.856 and BIC = -191.775. Based on these values, the 6-lag specification is preferred. Production data are from FAO, 1961–2022. Newey-West standard errors with one lag in parentheses. *** p<0.01, ** p<0.05, * p<0.1.

Table SI7: Long-run supply elasticity of oil palm

	Log quantity Q			Log area			Log yield		
	(1)	(2)	(3)	(4)	(5)	(6)	(7)	(8)	(9)
ΔP_{t-1}	0.0512	0.0380	0.00516	0.0302	0.0227	0.00729	0.0202	0.0146	-0.00267
	(0.0428)	(0.0411)	(0.0213)	(0.0271)	(0.0249)	(0.0205)	(0.0187)	(0.0201)	(0.00245)
ΔP_{t-2}	0.0432	0.0295	0.0118	0.0319	0.0254	0.0167	0.0118	0.00453	-0.00432**
	(0.0416)	(0.0398)	(0.0158)	(0.0236)	(0.0217)	(0.0153)	(0.0202)	(0.0209)	(0.00189)
ΔP_{t-3}	0.0798	0.0626	0.0315	0.0601**	0.0518**	0.0365*	0.0193	0.0105	-0.00517*
	(0.0522)	(0.0458)	(0.0220)	(0.0284)	(0.0244)	(0.0208)	(0.0267)	(0.0255)	(0.00289)
ΔP_{t-4}	0.0588	0.0411	0.0150	0.0457	0.0373	0.0242	0.0135	0.00411	-0.00869***
	(0.0546)	(0.0493)	(0.0223)	(0.0333)	(0.0318)	(0.0221)	(0.0251)	(0.0205)	(0.00269)
ΔP_{t-5}	0.104	0.108**	0.0629**	0.0896**	0.0898***	0.0678**	0.0148	0.0190	-0.00398
	(0.0616)	(0.0490)	(0.0275)	(0.0373)	(0.0311)	(0.0255)	(0.0276)	(0.0220)	(0.00332)
ΔP_{t-6}	0.0884	0.0882*	0.0485*	0.0762*	0.0746**	0.0551**	0.0126	0.0141	-0.00597*
	(0.0685)	(0.0514)	(0.0257)	(0.0401)	(0.0317)	(0.0234)	(0.0306)	(0.0229)	(0.00340)
Log palm oil price P_{t-7}	0.144*	0.174***	0.0965***	0.124**	0.133***	0.0962***	0.0201	0.0408*	0.000279
	(0.0744)	(0.0567)	(0.0335)	(0.0470)	(0.0373)	(0.0301)	(0.0301)	(0.0237)	(0.00390)
Shocks ω_t	0.827***	0.889***	0.809***	-0.192	-0.171*	-0.207***	0.0146	0.0552	0.0111
	(0.243)	(0.190)	(0.0603)	(0.134)	(0.0980)	(0.0554)	(0.113)	(0.0985)	(0.0105)
Observations	44	44	44	44	44	44	44	44	44
Knots	3	4	5	3	4	5	3	4	5

Long-run supply elasticity of oil palm with respect to palm oil prices. Model selection criteria for the 7-lag specification of the quantity regression with 5 spline knots are AIC = -200.387 and BIC = -177.192. For comparison, the 8-lag model yields AIC = -199.725 and BIC = -174.746, while the 5-lag model yields AIC = -193.808 and BIC = -172.398. Based on these criteria, the 7-lag specification is preferred. Production data are from FAS, 1976–2019. Newey-West standard errors with one lag in parentheses. *** p<0.01, ** p<0.05, * p<0.1.

Table SI8: Price effects on deforestation area for palm

	(1)	(2)	(3)
Palm revenue (t-1)	9.395***	9.322***	9.535***
	(1.260)	(1.256)	(1.217)
Observations	549,185	549,185	549,185
Cells	32,305	32,305	32,305
Time control	Country-year FE	Year FE	Forest cover trends

Robust standard errors clustered at the second administrative level
*** p<0.01, ** p<0.05, * p<0.1

Table SI9: Examination on reverse causality: dropping cells with a large palm plantation share

	W/O top 10% (1)	W/O top 25% (2)	W/O top 50% (3)
Palm revenue (t-1)	9.694***	9.786***	8.519***
	(1.224)	(1.171)	(0.989)
Observations	544,748	537,268	521,407
Cells	32,044	31,604	30,671
FE	Cell+County-year	Cell+County-year	Cell+County-year

Robust standard errors clustered at the second administrative level
*** p<0.01, ** p<0.05, * p<0.1

Table SI10: Price effects on deforestation area for palm controlling for weather

	(1)	(2)	(3)
Palm revenue (t-1)	9.963***	10.06***	9.895***
	(1.326)	(1.333)	(1.319)
Temperature	650.2***	279.6	578.7***
	(86.54)	(301.2)	(92.44)
Precipitation	0.0123	-2.094	-1.578
	(1.559)	(3.491)	(2.621)
Precipitation squared		0.486	
		(0.501)	
Temperature squared		175.9	
		(134.6)	
S.D. of temperature			9.436***
			(3.102)
S.D. of precipitation			0.445
			(0.570)
Observations	509,218	509,218	509,218
Cells	29,954	29,954	29,954
FE	Cell+County-year	Cell+County-year	Cell+County-year

Robust standard errors clustered at the second administrative level
*** p<0.01, ** p<0.05, * p<0.1

Table SI11: Addressing confounders from attainable yields: Price effects on deforestation area for palm

	AY X time trend	W/O AY>90th quantile	W/O AY<10th quantile	W/O AY<10th | >90th quantile
	(1)	(2)	(3)	(4)
Palm revenue (t-1)	12.07***	8.852***	10.14***	9.591***
	(1.684)	(1.340)	(1.371)	(1.461)
Observations	549,185	494,275	494,258	439,348
Cells	32,305	29,075	29,074	25,844
FE	Cell+County-year	Cell+County-year	Cell+County-year	Cell+County-year

Robust standard errors clustered at the second administrative level
*** p<0.01, ** p<0.05, * p<0.1

Table SI12: Price effects on deforestation area for palm considering prices from different periods

	(1)	(2)	(3)	(4)	(5)	(6)	(7)	(8)
Palm revenue	7.210***		-0.0990	0.477	0.691			
	(1.317)		(1.014)	(1.026)	(1.208)			
Palm revenue (t-1)		9.395***	9.455***	5.949***	5.704***			
		(1.260)	(1.106)	(1.125)	(1.238)			
Palm revenue (t-2)				3.785***	4.250***			
				(0.904)	(1.391)			
Palm revenue (t-3)					-0.480			
					(1.425)			
Mean of revenue (t-1 to t)						10.02***		
						(1.503)		
Mean of revenue (t-3 to t)							10.63***	
							(1.506)	
Mean of revenue (t-5 to t)								7.448***
								(1.565)
Cumulative effect	–	–	9.356***	10.211***	10.165***	–	–	–
Observations	549,185	549,185	549,185	549,185	549,185	549,185	549,185	549,185
Cells	32,305	32,305	32,305	32,305	32,305	32,305	32,305	32,305
FE	Cell+County-year	Cell+County-year	Cell+County-year	Cell+County-year	Cell+County-year	Cell+County-year	Cell+County-year	Cell+County-year

Robust standard errors clustered at the second administrative level
*** p<0.01, ** p<0.05, * p<0.1

Table SI13: Palm price deviation effects on deforestation area for palm

	(1)	(2)	(3)
Revenue deviation from past 5 years	9.415***		
	(1.536)		
Revenue deviation from past 7 years		9.425***	
		(1.424)	
Revenue deviation from past 10 years			10.51***
			(1.480)
Observations	549,185	549,185	549,185
Cells	32,305	32,305	32,305
FE	Cell+County-year	Cell+County-year	Cell+County-year

Robust standard errors clustered at the second administrative level
*** p<0.01, ** p<0.05, * p<0.1

Table SI14: Comparison of carbon emission estimates (Mg CO_2e/ha) from land-use change across studies

Study	Biomass	SOC	Peatland	Palm sequestration	Total	Notes
Our estimate	438.19	54.84	355.04	-219.84	628.24	
Guillaume et al. (2018)(45)	756.98	39.94	–	-160.85	636.07	The study was conducted in Jambi Province, central Sumatra, Indonesia, across 32 plots comparing carbon stocks under different land uses, from rainforest to plantations. Their estimated biomass is higher, likely because their baseline forest is restricted to rainforest. Biomass varies widely across regions and forest types, so studies focusing only on rainforest are expected to report higher values than our estimates, which are based on 30 m resolution biomass data. Emissions from peatland decomposition are not considered in their study.
Carlson et al. (2013)(44)	749.45	–	131.17	-103.69	776.93	This study focuses on Kalimantan, Indonesia, from 1990 to 2010. Forest loss is classified by type (intact, logged, agroforest), but a single AGB value is applied to each category without accounting for local variation due to climate or geography. These methodological choices, along with differences in study period and coverage, likely explain the higher AGB estimate relative to ours. For peatland, they assume only ten years of drainage emissions; if extended to the full oil palm lifecycle, assuming the same emission per year, their implied peatland emissions (327.92 Mg CO_2e/ha) are close to ours. Remaining differences may reflect study scope and timing, which affect the extent of peatland conversion considered. They do not account for SOC from non-peat soils.
Busch et al. (2015)(42)	749.93			–	749.93	This study examines deforestation in Indonesia from 2000 to 2010, covering palm expansion as well as other drivers such as logging. Biomass and peat data are applied to the exact deforestation locations. Their estimate (749.93 Mg CO_2e/ha, including biomass, SOC, and peatland decomposition) is close to our estimate of 848.08 Mg CO_2e/ha, supporting our use of spatially explicit data on biomass and peatland transitions. Remaining differences likely reflect study period, geographic scope, and their inclusion of non-palm deforestation. They do not account for carbon sequestered by replanted trees.
Groom et al. (2022)(43)	570.12	–	–	–	570.12	This estimate focuses on primary and peatland forests that avoided deforestation during Indonesia's moratorium on new forest concessions (2011–2017). Their biomass estimates are based on exact deforestation locations and are close to—but higher than—ours (438.19 Mg CO_2e/ha). The higher values likely reflect differences in forest types: our study also includes managed natural forests, planted forests, and agroforestry, which generally have lower biomass than primary forests. Differences in study period and geographic scope may also contribute. Emissions from SOC and peatland decomposition, and carbon sequestered by replanted trees are not considered in their study.

For studies reporting emissions in terms of carbon (C), we convert to CO_2 by multiplying the carbon mass by 3.664.

Table SI15: Demand flexibility – sensitivity checks of yield shock construction

	Baseline: Yield trend with 5 knots			Yield trend with 3 knots			Yield trend with 4 knots		
	(1)	(2)	(3)	(4)	(5)	(6)	(7)	(8)	(9)
Log oil crops q_t	-2.271*	-2.733**	-3.459***	-2.743*	-3.675***	-3.535***	-3.167**	-3.098***	-3.179***
	(1.286)	(1.172)	(1.062)	(1.420)	(1.271)	(1.098)	(1.233)	(1.137)	(0.991)
First stage									
Shocks ω	1.171***	1.204***	1.190***	1.019***	1.123***	1.134***	1.269***	1.267***	1.256***
	(0.185)	(0.199)	(0.209)	(0.171)	(0.203)	(0.199)	(0.201)	(0.201)	(0.199)
Observations	62	62	62	62	62	62	62	62	62
R-squared	0.497	0.520	0.579	0.475	0.459	0.575	0.451	0.499	0.595
Effective F	39.95	36.46	32.41	35.46	30.46	32.48	40.00	39.85	39.76
Knots	3	4	5	3	4	5	3	4	5

Production data are from FAO, 1961–2022. Robust standard errors in parentheses. *** $p < 0.01$, ** $p < 0.05$, * $p < 0.1$.

Table SI16: Short-run supply elasticity for palm – sensitivity checks of yield shock construction

	Baseline: Yield trend with 5 knots			Yield trend with 3 knots			Yield trend with 4 knots		
	(1)	(2)	(3)	(4)	(5)	(6)	(7)	(8)	(9)
Log palm oil price P_{t-1}	0.0300	0.0252	0.00526	0.00291	0.0109	0.00726	0.0177	0.00761	0.00620
	(0.0339)	(0.0347)	(0.0156)	(0.0208)	(0.0223)	(0.0149)	(0.0191)	(0.0188)	(0.0152)
Shocks ω_t	0.767***	0.772***	0.750***	0.976***	0.967***	0.772***	0.959***	0.946***	0.759***
	(0.229)	(0.218)	(0.0805)	(0.0706)	(0.0739)	(0.0745)	(0.0659)	(0.0543)	(0.0781)
Observations	44	44	44	44	44	44	44	44	44
Knots	3	4	5	3	4	5	3	4	5

Production data are from FAS, 1976–2019. Newey–West standard errors with one lag in parentheses. *** $p < 0.01$, ** $p < 0.05$, * $p < 0.1$.

Table SI17: Short-run supply elasticity for other oil crops – sensitivity checks of yield shock construction

	Baseline: Yield trend with 5 knots			Yield trend with 3 knots			Yield trend with 4 knots		
	(1)	(2)	(3)	(4)	(5)	(6)	(7)	(8)	(9)
Log palm oil price P_{t-1}	0.0710***	0.0590***	0.0614***	0.0815***	0.0715***	0.0625***	0.0860***	0.0700***	0.0572***
	(0.0213)	(0.0193)	(0.0191)	(0.0208)	(0.0187)	(0.0187)	(0.0201)	(0.0181)	(0.0182)
Shocks ω_t	1.314***	1.275***	1.280***	1.213***	1.187***	1.190***	1.303***	1.287***	1.306***
	(0.115)	(0.113)	(0.124)	(0.115)	(0.119)	(0.118)	(0.126)	(0.123)	(0.117)
Observations	62	62	62	62	62	62	62	62	62
Knots	3	4	5	3	4	5	3	4	5

Production data are from FAO, 1961–2022. Newey–West standard errors with one lag in parentheses. *** $p < 0.01$, ** $p < 0.05$, * $p < 0.1$.

Table SI18: Long-run supply elasticity for palm – sensitivity checks of yield shock construction

	Baseline: Yield trend with 5 knots			Yield trend with 3 knots			Yield trend with 4 knots		
	(1)	(2)	(3)	(4)	(5)	(6)	(7)	(8)	(9)
ΔP_{t-1}	0.0512	0.0380	0.00516	0.0133	0.0129	0.00571	0.0193	0.00951	0.00578
	(0.0428)	(0.0411)	(0.0213)	(0.0285)	(0.0267)	(0.0209)	(0.0286)	(0.0233)	(0.0210)
ΔP_{t-2}	0.0432	0.0295	0.0118	0.0128	0.0139	0.0140	0.0224	0.0120	0.0128
	(0.0416)	(0.0398)	(0.0158)	(0.0263)	(0.0246)	(0.0157)	(0.0268)	(0.0199)	(0.0155)
ΔP_{t-3}	0.0798	0.0626	0.0315	0.0337	0.0361	0.0335	0.0471	0.0331	0.0327
	(0.0522)	(0.0458)	(0.0220)	(0.0299)	(0.0280)	(0.0213)	(0.0338)	(0.0247)	(0.0217)
ΔP_{t-4}	0.0588	0.0411	0.0150	0.0445	0.0388	0.0194	0.0546*	0.0315	0.0169
	(0.0546)	(0.0493)	(0.0223)	(0.0312)	(0.0310)	(0.0220)	(0.0311)	(0.0265)	(0.0220)
ΔP_{t-5}	0.104	0.108**	0.0629**	0.0840**	0.0851***	0.0630**	0.0786**	0.0761***	0.0632**
	(0.0616)	(0.0490)	(0.0275)	(0.0335)	(0.0301)	(0.0262)	(0.0375)	(0.0272)	(0.0269)
ΔP_{t-6}	0.0884	0.0882*	0.0485*	0.0724**	0.0713**	0.0488*	0.0700*	0.0624**	0.0487*
	(0.0685)	(0.0514)	(0.0257)	(0.0339)	(0.0302)	(0.0241)	(0.0400)	(0.0266)	(0.0250)
Log palm oil price P_{t-7}	0.144*	0.174***	0.0965***	0.124***	0.128***	0.0918***	0.0952*	0.114***	0.0949***
	(0.0744)	(0.0567)	(0.0335)	(0.0434)	(0.0376)	(0.0318)	(0.0485)	(0.0344)	(0.0327)
Shocks ω_t	0.827***	0.889***	0.809***	1.080***	1.018***	0.820***	0.993***	0.967***	0.813***
	(0.243)	(0.190)	(0.0603)	(0.0791)	(0.0716)	(0.0564)	(0.0821)	(0.0583)	(0.0589)
Observations	44	44	44	44	44	44	44	44	44
Knots	3	4	5	3	4	5	3	4	5

Production data are from FAS, 1976–2019. Newey–West standard errors with one lag in parentheses. *** $p < 0.01$, ** $p < 0.05$, * $p < 0.1$.

Table SI19: Long-run supply elasticity for other oil crops – sensitivity checks of yield shock construction

	Baseline: Yield trend with 5 knots			Yield trend with 3 knots			Yield trend with 4 knots		
	(1)	(2)	(3)	(4)	(5)	(6)	(7)	(8)	(9)
ΔP_{t-1}	0.0806***	0.0832***	0.0841***	0.0881***	0.0939***	0.0823***	0.0880***	0.0918***	0.0816***
	(0.0191)	(0.0185)	(0.0228)	(0.0184)	(0.0186)	(0.0222)	(0.0183)	(0.0183)	(0.0222)
ΔP_{t-2}	0.0391	0.0397	0.0402	0.0466*	0.0493**	0.0379	0.0457*	0.0471*	0.0369
	(0.0268)	(0.0256)	(0.0268)	(0.0245)	(0.0233)	(0.0248)	(0.0253)	(0.0242)	(0.0262)
ΔP_{t-3}	0.0635*	0.0637**	0.0647**	0.0840***	0.0862***	0.0632**	0.0794**	0.0803***	0.0601*
	(0.0334)	(0.0311)	(0.0316)	(0.0301)	(0.0276)	(0.0307)	(0.0302)	(0.0281)	(0.0307)
ΔP_{t-4}	0.0747***	0.0789***	0.0802***	0.0875***	0.0965***	0.0762***	0.0847***	0.0904***	0.0727***
	(0.0178)	(0.0152)	(0.0212)	(0.0200)	(0.0180)	(0.0224)	(0.0186)	(0.0167)	(0.0218)
ΔP_{t-5}	0.0797**	0.0829***	0.0843**	0.0937***	0.101***	0.0802**	0.0894***	0.0940***	0.0756**
	(0.0307)	(0.0287)	(0.0322)	(0.0346)	(0.0324)	(0.0336)	(0.0323)	(0.0307)	(0.0320)
Log palm oil price P_{t-6}	0.118***	0.130***	0.133***	0.128***	0.150***	0.128***	0.125***	0.140***	0.121***
	(0.0212)	(0.0214)	(0.0282)	(0.0240)	(0.0253)	(0.0294)	(0.0227)	(0.0240)	(0.0285)
Shocks ω_t	1.325***	1.316***	1.311***	1.178***	1.190***	1.265***	1.240***	1.242***	1.305***
	(0.129)	(0.128)	(0.130)	(0.127)	(0.122)	(0.129)	(0.128)	(0.125)	(0.130)
Observations	57	57	57	57	57	57	57	57	57
Knots	3	4	5	3	4	5	3	4	5

Production data are from FAO, 1966–2022. Newey–West standard errors with one lag in parentheses. *** $p < 0.01$, ** $p < 0.05$, * $p < 0.1$.